RESEARCH PAPER

Rho kinase inhibitor fasudil reduces L-DOPA-induced dyskinesia in a rat model of Parkinson's disease

Andrea Lopez-Lopez[1,2] 🄳 | Carmen M. Labandeira[1,3] 🄳 |
Jose L. Labandeira-Garcia[1,2] 🄳 | Ana Muñoz[1,2] 🄳

[1]Laboratory of Cellular and Molecular Neurobiology of Parkinson's Disease, Research Center for Molecular Medicine and Chronic Diseases (CIMUS), Department of Morphological Sciences, IDIS, University of Santiago de Compostela, Santiago de Compostela, Spain

[2]Networking Research Center on Neurodegenerative Diseases (CiberNed), Madrid, Spain

[3]Department of Clinical Neurology, Hospital Alvaro Cunqueiro, University Hospital Complex, Vigo, Spain

Correspondence
Jose L. Labandeira-Garcia, M.D., Ph.D., and Ana M. Muñoz, Ph.D., Department of Morphological Sciences, Faculty of Medicine, University of Santiago de Compostela, 15782 Santiago de Compostela, Spain.
Email: joseluis.labandeira@usc.es; anamaria.munoz@usc.es

Funding information
Consellería de Cultura, Educación e Ordenación Universitaria, Xunta de Galicia, Grant/Award Numbers: ED431G/05, ED431C 2018/10; European Regional Development Fund; Instituto de Salud Carlos III, Grant/Award Number: RD16/0011/0016; Secretaría de Estado de Investigación, Desarrollo e Innovación, Grant/Award Number: RTI2018-098830-B-I00

Background and Purpose: Rho kinase (ROCK) activation is involved in neuro-inflammatory processes leading to progression of neurodegenerative diseases such as Parkinson's disease. Furthermore, ROCK plays a major role in angiogenesis. Neuroinflammation and angiogenesis are mechanisms involved in developing L-DOPA-induced dyskinesias (LID). However, it is not known whether ROCK plays a role in LID and whether ROCK inhibitors may be useful against LID.

Experimental Approach: In rats, we performed short- and long-term dopaminergic lesions using 6-hydroxydopamine and developed a LID model. Effects of dopaminergic lesions and LID on the RhoA/ROCK levels were studied by western blot, real-time PCR analyses and ROCK activity assays in the substantia nigra and striatum. The effects of the ROCK inhibitor fasudil on LID were particularly investigated.

Key Results: Short-term 6-hydroxydopamine lesions increased nigrostriatal RhoA/ROCK expression, apparently related to the active neuroinflammatory process. However, long-term dopaminergic denervation (completed and stabilized lesions) led to a decrease in RhoA/ROCK levels. Rats with LID showed a significant increase of RhoA and ROCK expression. The development of LID was reduced by the ROCK inhibitor fasudil (10 and 40 mg·kg^{-1}), without interfering with the therapeutic effect of L-DOPA. Interestingly, treatment of 40 mg·kg^{-1} of fasudil also induced a significant reduction of dyskinesia in rats with previously established LID.

Conclusion and Implications: The present results suggest that ROCK is involved in the pathophysiology of LID and that ROCK inhibitors such as fasudil may be a novel target for preventing or treating LID. Furthermore, previous studies have revealed neuroprotective effects of ROCK inhibitors.

KEYWORDS
angiogenesis, dopamine, neuroinflammation, nigra, Parkinson, RhoA, ROCK, striatum

---

Abbreviations: 6-OHDA, 6-hydroxydopamine; AIMs, abnormal involuntary movements; AT1, angiotensin type-1 receptor; BBB, blood–brain barrier; LID, L-DOPA-induced dyskinesia; MFB, medial forebrain bundle; PD, Parkinson's disease; ROCK, Rho kinase.

1 | INTRODUCTION

Parkinson's disease (PD) is a major neurodegenerative disease, which is characterized by the progressive loss of dopaminergic neurons in the substantia nigra. Dopamine replacement therapy using the precursor L-DOPA is the main treatment. However, abnormal involuntary movements (AIMs) known as dyskinesias are one of the most important complications of chronic L-DOPA treatment. These movements are characterized by chorea in many cases or dystonia occasionally, and the most frequent clinical presentation is the peak of dose dyskinesia. The pathophysiology of L-DOPA-induced dyskinesia (LID) is not fully understood. In neurotoxin animal models of PD, the expression of involuntary movements is also observed shortly after the administration of L-DOPA (Cenci & Crossman, 2018). The classical PD model in rodents is induced by injection of 6-hydroxydopamine (6-OHDA) close to the dopaminergic neurons, which induces dopaminergic degeneration (Rodriguez-Pallares et al., 2007; Soto-Otero, Méndez-Alvarez, Hermida-Ameijeiras, Muñoz-Patiño, & Labandeira-Garcia, 2000). Different factors appear to be involved in L-DOPA-induced dyskinesia, which increases the difficulty in developing efficient treatments (Johnston et al., 2019). Abnormal activity of the corticostriatal synapses (Cenci & Konradi, 2010), the unregulated release of dopamine by the 5-HTergic terminals (Muñoz et al., 2008) and NO (Bortolanza et al., 2015; Padovan-Neto, Cavalcanti-Kiwiatkoviski, Carolino, Anselmo-Franci, & Del Bel, 2015) have been related to L-DOPA-induced dyskinesia. Recent evidences have shown that factors such as neuroinflammation (Barnum et al., 2008; Mulas et al., 2016; Pisanu et al., 2018; Teema, Zaitone, & Moustafa, 2016) and angiogenesis (Lerner et al., 2017; Ohlin et al., 2011) also play a major role in L-DOPA-induced dyskinesia. Consistent with this, animal models of L-DOPA-induced dyskinesia and PD patients showed increased levels of vascular endothelial growth factor (VEGF) and inflammatory cytokines such as IL-1β (Barnum et al., 2008; Muñoz, Garrido-Gil, Dominguez-Meijide, & Labandeira-Garcia, 2014; Ohlin et al., 2011; Teema et al., 2016).

Interestingly, RhoA initiates cellular processes that act on its direct effector Rho kinase (ROCK), which plays a critical role in the neuroinflammatory response including functions related to actin cytoskeleton as microglial migration (Labandeira-Garcia et al., 2015; Villar-Cheda et al., 2012). The RhoA/ROCK pathway is also involved in regulation of angiogenesis and microvascular permeability (Bryan et al., 2010). In addition, ROCK possesses multiple substrates and modulation of ROCK activity has been suggested as a neuroprotective treatment for several diseases including PD (Barcia et al., 2012; Labandeira-Garcia et al., 2015; Moskal et al., 2020; Tatenhorst et al., 2014; Villar-Cheda et al., 2012). Interestingly, ROCK inhibitors, such as fasudil, are currently used against vascular diseases in clinical practice in several countries (Koch et al., 2018). However, the possible involvement of the RhoA/ROCK in L-DOPA-induced dyskinesia development or whether ROCK inhibitors may become a new therapeutical strategy against L-DOPA-induced dyskinesia have not been investigated, which was studied in the present experiments using a 6-OHDA rat model of L-DOPA-induced dyskinesia and the ROCK inhibitor fasudil.

What is already known

- Rho kinase activation mediates neuroinflammation and angiogenesis, which are involved in development of L-DOPA-induced dyskinesias.
- Current dyskinesia treatment is disappointing and several suggested drugs converge on Rho kinase regulation.

What this study adds

- Dopaminergic lesions and dyskinesia modify Rho kinase (ROCK) activity in the nigra and striatum.
- The ROCK inhibitor fasudil inhibits development and reduces already established L-DOPA-induced dyskinesia (LID).

What is the clinical significance

- Fasudil, already used against vascular diseases, is a good candidate for the treatment of dyskinesias.
- Fasudil does not affect therapeutic effect of L-DOPA and has previously shown dopaminergic neuroprotective properties.

2 | METHODS

2.1 | Experimental design

Animal studies are reported in compliance with the ARRIVE guidelines (Percie du Sert et al., 2020) and with the recommendations made by the *British Journal of Pharmacology* (Lilley et al., 2020). Adult female Sprague–Dawley rats (RGD Cat# 68140, RRID:RGD_68140; weighing 225–250 g at the beginning of the experiments; 10 weeks old) were used. Initially, groups of equal size were designed using randomization and blinded analysis. Female rats were used because the important increase in body weight of male rats in long-term experiments may affect motor behavioural tests and all rats selected for the experiments already had maximal dopaminergic denervation (i.e. levels of dopaminergic denervation will not be influenced oestrogen levels). Rats were pair-housed under a 12-h light/dark cycle and with ad libitum access to food and water. Behavioural testing was initiated at the beginning of the dark cycle. All experiments were carried out in accordance with the European Communities Council Directive 2010/63/EU, Directive 86/609/EEC and Spanish RD 526/2014 and were approved by the corresponding committee at the University of Santiago de Compostela. Four groups of experiments (*I–IV*; *n* = 207) were carried out (Figure 1). In *Experiment I*, we studied the effect of dopaminergic lesions on RhoA and ROCK levels.
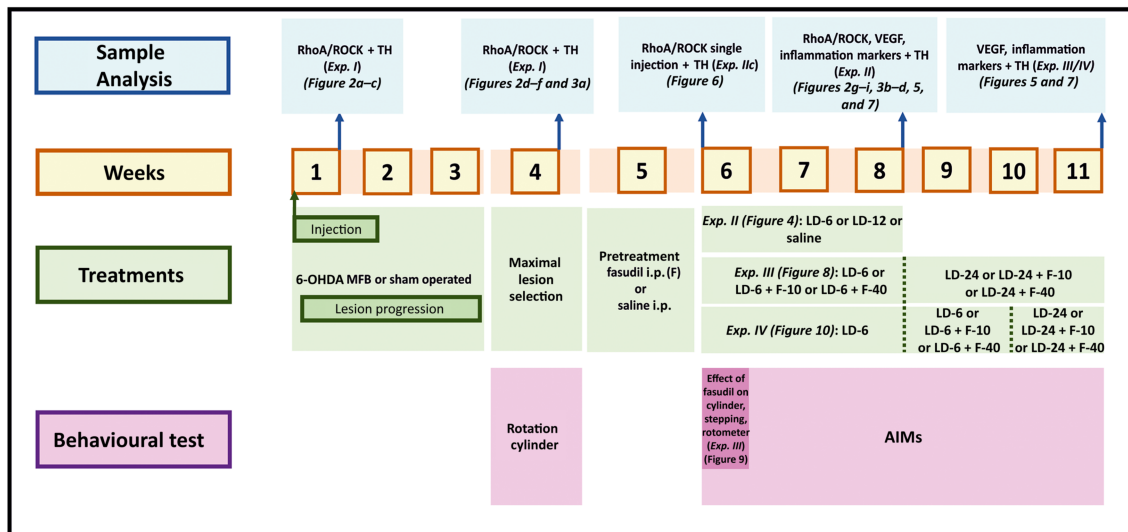
FIGURE 1 Experimental design (Weeks 1–11). Time course of experiments (I–IV), sample analysis and behavioural tests. AIMs, abnormal involuntary movements; Exp., experiment; F, fasudil; LD, L-DOPA; MFB, medial forebrain bundle

We used rats injected with 6-OHDA in the medial forebrain bundle (MFB; see Section 2.2) and killed rats 1 week ($n = 12$; Group Ia), 4 weeks ($n = 12$, Group Ib) or 8 weeks ($n = 12$; Group Ic) after lesion to observe levels of ROCK during the acute period of the 6-OHDA lesion characterized by neuronal death and neuroinflammation, when the lesion is complete and stabilized and when these rats can be compared with dyskinetic rats treated with L-DOPA for 3 weeks (see below), respectively. Sham-operated rats (i.e. injected with vehicle close to the MFB: sterile saline containing 0.2% ascorbic acid) with normal dopaminergic innervation were used as controls ($n = 12$ per group). In *Experiment II*, we used rats with maximal unilateral 6-OHDA lesions to investigate the effects of L-DOPA on development of dyskinesia and RhoA/ROCK expression. Considering the time course of the 6-OHDA lesion, which is stabilized 3–4 weeks after the toxin injection (Labandeira-Garcia, Rozas, Lopez-Martin, Liste, & Guerra, 1996), rats with maximal dopaminergic lesions were selected by behavioural tests performed during the fourth week (see Sections 2.3.1 and 2.3.2). Rats with maximal lesions were allocated into well-matched subgroups before L-DOPA treatment according to the **amphetamine** rotation to exclude any possible difference in dopaminergic lesion between experimental groups. L-DOPA treatment was initiated 6 weeks after the 6-OHDA injection. L-DOPA was daily injected by subcutaneous administration until induction of consistent levels of AIMs was achieved (i.e. Weeks 6, 7 and 8 after 6-OHDA injection). L-DOPA doses of 6 mg·kg^{-1} ($n = 16$; Group IIa) or 12 mg·kg^{-1} ($n = 12$; Group IIb) in saline were used, together with **benserazide** (10 mg·kg^{-1}) as a peripheral DOPA decarboxylase inhibitor. Dyskinetic behaviour was tested periodically using an AIMs scale (see Section 2.3.4) and the animals were finally killed for post-mortem studies (see Sections 2.4–2.7). An additional group of rats (Group IIc) received a single injection of L-DOPA (12 mg·kg^{-1}) to analyse the acute effect of L-DOPA on dyskinesia and ROCK activation and the rats were killed 1 h ($n = 7$) or 4 h ($n = 7$)

after that single injection. The corresponding controls were 6-OHDA-lesioned rats injected with saline instead of L-DOPA ($n = 12$ and 7, respectively). A few rats treated with 6 mg·kg^{-1} of L-DOPA did not develop dyskinesia brain tissue from these rats (Group IId; $n = 7$) together with the corresponding controls ($n = 16$) were processed to investigate possible effects of L-DOPA on ROCK activity independently of development of dyskinesia. In *Experiment III*, we assessed the effect of ROCK inhibitor fasudil on the development of L-DOPA-induced dyskinesia. Two groups of 6-OHDA-lesioned rats (matched on the basis of their amphetamine-induced rotation scores) were treated with L-DOPA (6 mg·kg^{-1}·day^{-1}; s.c. plus 10 mg·kg^{-1} of benserazide) for 3 weeks (Weeks 6–8 after 6-OHDA). One group of rats was treated with the ROCK inhibitor fasudil (10 mg·kg^{-1}·day^{-1}, in saline, i.p.; LC laboratories) for 5 days before the first L-DOPA injection (i.e. during the fifth week after 6-OHDA) and then 30 min before each L-DOPA injection ($n = 10$; Group IIIa) to study effects of L-DOPA in the presence of already established ROCK inhibition and the other group of animals was treated with saline (instead of fasudil) + L-DOPA ($n = 9$; Group IIIb). Peripherally administered fasudil can cross the blood–brain barrier (BBB) (Zhang, Gao, Huang, & Xu, 2009) showing effects on the CNS in many previous studies (see for review Koch et al., 2018; Labandeira-Garcia et al., 2015). The initial dose of fasudil was the lowest dose that resulted neuroprotective in our previous studies (Rodriguez-Perez, Borrajo, Rodriguez-Pallares, Guerra, & Labandeira-Garcia, 2015). An additional group of rats was treated as in IIIa using higher dose of fasudil (40 mg·kg^{-1}·day^{-1}, i.p.; $n = 7$; Group IIIc). The corresponding controls were treated with saline + L-DOPA as in Group IIIb ($n = 7$; Group IIId). After the 3-week period of treatment (Weeks 6–8 after 6-OHDA) with 6 mg·kg^{-1} (i.e. on the ninth week after 6-OHDA injection), the L-DOPA dose was increased up to 24 mg·kg^{-1} to investigate if fasudil could be effective in reducing high levels of L-DOPA-induced dyskinesia.

Cylinder, stepping and rotameter tests were performed to evaluate whether treatment with fasudil (10 or 40 mg·kg^{-1}·day^{-1}) may affect the therapeutic effect of L-DOPA. The motor behaviour was analysed at the beginning of the L-DOPA treatment (on the sixth week post-6-OHDA; after two, four and six L-DOPA injections, for cylinder, stepping and rotameter, respectively) to prevent possible interference of L-DOPA-induced dyskinesia with the performance of the behavioural tests. Finally, *Experiment IV* was designed to investigate whether ROCK inhibition could reverse dyskinesias in L-DOPA-primed animals (i.e. once the L-DOPA-induced dyskinesia was consistently established). Rats were first injected with L-DOPA only (6 mg·kg^{-1}·day^{-1}, s.c.; plus 10 mg·kg^{-1} of benserazide; *n* = 16) for 3 weeks (Weeks 6–8 after 6-OHDA injection, as above). Once L-DOPA-induced dyskinesia was established, groups of rats (IVa–d) were matched on the basis of their dyskinesia scores. Then (on Weeks 9 and 10 after 6-OHDA lesion) a first group of rats was treated with L-DOPA (6 mg·kg^{-1}·day^{-1}) and 10 mg·kg^{-1}·day^{-1} of fasudil (i.p.; *n* = 8; Group IVa) or L-DOPA + saline (*n* = 8; Group IVb) and the dyskinetic behaviour was analysed. A second group of dyskinetic animals was treated (on Weeks 9 and 10 after 6-OHDA injection) with L-DOPA (6 mg·kg^{-1}·day^{-1}) and 40 mg·kg^{-1}·day^{-1} of fasudil (i.p.; *n* = 9; Group IVc) and dyskinesia was compared with the corresponding controls treated with L-DOPA + saline (*n* = 9; Group IVd). After this second period of treatment (i.e. on the 11th week post-6-OHDA), the dose of L-DOPA was increased to 24 mg·kg^{-1}·day^{-1} to enhance levels of dyskinesia in the same rats and to know if simultaneous treatment with fasudil (as above) was able to inhibit higher levels of dyskinesia. Tests were performed by an experimentally blinded investigator.

At the end of the experiments, rats were stunned with carbon dioxide and then killed by decapitation (90 min after the last L-DOPA injection; 1 or 4 h after the single L-DOPA injection in Experiment IIc). The whole substantia nigra region and the whole striatum were rapidly dissected on an ice bath, frozen in dry ice and stored at −80°C until processed for western blot, ROCK activity assay and real-time quantitative RT-PCR. Values were obtained from the lesioned side and compared with the corresponding area of the control group. Rats not used for RT-PCR, western blot or ROCK activity were killed by an overdose of chloral hydrate and perfused for confirmation of maximal lesions by tyrosine hydroxylase (TH) immunohistochemistry of dopaminergic neurons in the substantia nigra and dopaminergic terminals in the striatum.

2.2 | 6-OHDA lesion of the dopaminergic system

Rats were deeply anaesthetized with a mixture of ketamine (50 mg·kg^{-1})/medetomidine (0.4 mg·kg^{-1}) and mounted in a stereotaxic frame (Kopf Instruments). Subcutaneous buprenorphine (0.05 mg·kg^{-1}) was administered for analgesia at the end of surgery, immediately after the incision was closed and before the rat regained consciousness. A second dose was administered 12 h later. Lesions were performed in the right MFB to achieve complete lesion of the nigrostriatal pathway. The rats were injected with 12 μg of 6-OHDA

(to provide 8 μg of 6-OHDA free base; Sigma) in 4 μl of sterile saline containing 0.2% ascorbic acid. The stereotaxic coordinates were 3.7 mm posterior to bregma, 1.6 mm lateral to midline and 8.8 mm ventral to the skull at the midline, in the flat skull position. The tooth bar was set at −3.3 mm. The solution was injected using a 5-μl Hamilton syringe coupled to a motorized injector (Stoelting), at a rate of 0.5 μl·min^{-1}; the cannula was left in situ 2 min after injection. On the fourth week after 6-OHDA injection, the efficacy of the lesion was evaluated with the amphetamine rotation test and the cylinder test (see below). All rats showing maximal dopaminergic denervation were included in the study (i.e. no rat with complete denervation was excluded). The extent of the lesion was finally verified by TH western blot or immunohistochemistry analysis.

2.3 | Behavioural analysis

2.3.1 | Amphetamine- and L-DOPA-induced rotation

Amphetamine-induced rotation was performed on the fourth week after the 6-OHDA injection to evaluate the extent of the dopaminergic lesion. Turning behaviour was recorded in an automated rotameter (Rota-Count 8, Columbus Instruments, Columbus, USA). Right and left full body turns were recorded over 90 min after a 2.5 mg·kg^{-1} i.p. injection of D-amphetamine dissolved in saline. Animals rotating more than six net full turns per minute in the direction ipsilateral to the lesion were used in this study (i.e. those corresponding to more than 90% depletion of dopamine fibre terminals in the striatum) (Winkler, Kirik, Bjorklund, & Cenci, 2002). In *Experiment III*, rats were tested for evaluation of L-DOPA-induced rotation and effect of fasudil on motor activation induced by L-DOPA. Data were expressed as net full body turns per minute.

2.3.2 | Cylinder test

The cylinder test was used to evaluate forelimb akinesia and the efficacy of the lesion (Schallert & Tillerson, 1999). Rats were placed individually and videotaped in a transparent glass cylinder (20-cm diameter) with two mirrors to allow visualization from all directions and observation of the animals when they were turned away. The animals were then allowed to move freely in the cylinder and to explore the environment. An observer blinded to the treatment of the rats counted the number of weight-bearing touches made with each forelimb until a total of 20 touches. The data were expressed as per cent of touches with the lesioned paw relative to total. A normal symmetric animal would thus receive a score of 50% (indicated as a dashed line in the corresponding figures), whereas lesions usually reduce performance of the impaired paw to less than 20% of total wall counts. This test was also used to assess the influence of fasudil on the therapeutic effect of L-DOPA (*Experiment III*). At each test session, a new baseline value was obtained off-drug before any injection and rats were tested

again 90 min after L-DOPA injection. Fasudil was given 30 min prior to L-DOPA.

2.3.3 | Stepping test

The stepping test was used as an index of the therapeutic effect of L-DOPA. The stepping test was performed as described in detail previously (Olsson, Nikkhah, Bentlage, & Bjorklund, 1995) with minor modifications. Briefly, the rat was held by the experimenter fixing its hindlimbs with one hand and the forelimb not to be monitored with the other, while the unrestrained forepaw was touching the table. The number of adjusting steps was counted, while the rat was moving around the surface (90 cm in 5 s), in the forehand and backhand direction, for both forelimbs. The animals were habituated to the handling procedure for a week before testing. Values are reported as the sum of the steps in the forehand and backhand direction for both paws. Performance of the animals in the stepping test was assessed in the animals treated with both L-DOPA + fasudil (10 and 40 mg·kg^{-1}), L-DOPA + saline and 6-OHDA + saline (Experiment III; on the sixth week after 6-OHDA injection; Day 4 of treatment). The baseline stepping test was performed just before (about 5 min) the fasudil or saline injection. Then (30 min later) rats were injected with L-DOPA or saline and the stepping test was performed again 90 min after this second injection.

2.3.4 | L-DOPA-induced dyskinesia

The present model (rats with maximal unilateral dopaminergic lesions) is the usual model for investigation on dyskinesia in rodents (Cenci & Crossman, 2018). In order to induce L-DOPA-induced dyskinesia, L-DOPA (6, 12 or 24 mg·kg^{-1}; see above) was administered daily to each rat as a subcutaneous injection. L-DOPA was combined with the peripheral DOPA decarboxylase inhibitor benserazide (10 mg·kg^{-1}) dissolved in saline. L-DOPA-induced dyskinesia were evaluated according to a rat dyskinesia scale described in detail previously (Muñoz et al., 2014). Briefly, the animals were placed in individual transparent plastic cages without bedding material and were scored every 20 min after the injection of L-DOPA and for the entire time course of dyskinesias. The AIMs were classified into four subtypes according to their topographic distribution as limb, orolingual, axial and locomotive movement. The forelimb and orolingual dyskinesia are predominantly seen as hyperkinesia, while the axial dyskinesia is essentially a dystonic movement. Enhanced manifestations of normal behaviours, such as grooming, gnawing, rearing and sniffing, were not included in the rating. The severity of each AIM subtype was assessed using scores from 0 to 4 (1: occasional, i.e. present <50% of the time; 2: frequent, i.e. present >50% of the time; 3: continuous, but interrupted by strong sensory stimuli; 4: continuous, not interrupted by strong sensory stimuli). Integrated total AIMs score (raw data plot of total scores: axial + limb + orolingual AIM scores multiplied by the interval of observation: × 20 min) and total AIMs and

each AIM subtype were presented as time course curve and total AUC. Time course analysis for a single L-DOPA injection was represented showing the scores of the animals in each time point every 20 min.

2.4 | Western Blot and ELISA analysis

The Immuno-related procedures used comply with the recommendations made by the *British Journal of Pharmacology* (Alexander et al., 2018). Tissue from the substantia nigra area and striatum was homogenized in RIPA buffer containing protease inhibitor cocktail (Sigma). Tissue lysates were centrifuged and protein concentrations were quantified using the Pierce BCA Protein Assay Kit (Thermo Scientific, Fremont, CA, USA). Equal amounts of protein (25 μg) were separated by 5%–10% Bis-Tris polyacrylamide gel and transferred to nitrocellulose membranes (1620115, Bio-Rad, 0.45 μm). Precision standard plus (161-0374; Bio-Rad) was used as an MW marker. The membranes were incubated overnight with the following primary antibodies: mouse anti-ROCK II (Santa Cruz Biotechnology Cat# sc-398519; 1:200), mouse anti-RhoA (Santa Cruz Biotechnology Cat# sc-418, RRID:AB_628218; 1:200), mouse anti-VEGF (Santa Cruz Biotechnology Cat# sc-7269, RRID:AB_628430; 1:200) and hamster anti-IL-1β (Santa Cruz Biotechnology Cat# sc-12742, RRID:AB_627791; 1:100). Antibodies were diluted in 5% nonfat dry milk PBS 0.1% Tween 20. Mouse anti-TH antibody (Sigma-Aldrich Cat# T2928, RRID:AB_477569; 1:5,000) was also used to confirm the dopamine denervation. The membranes were incubated with the following HRP-conjugated secondary antibody rabbit anti-mouse (Agilent Cat# P0260, RRID:AB_2636929; 1:2,500) from Dako or mouse anti-Armenian hamster (Santa Cruz Biotechnology Cat# sc-2789, RRID:AB_628484; 1:2,500). Immunoreactive bands were detected with an Immun-Star HRP Chemiluminescent Kit (170-5044; Bio-Rad) and visualized with a chemiluminescence detection system (Molecular Imager ChemiDoc XRS System; Bio-Rad). Blots were stripped and reproved for anti-GAPDH (Sigma-Aldrich Cat# G9545, RRID:AB_796208; 1:25,000) as loading control. For each animal, protein expression was measured by densitometry of the corresponding band and expressed relative to the GAPDH band value. The data were then normalized to the values of the control group of the same batch (100%) to counteract any between-batch variability. Finally, the results were expressed as mean ± SEM.

For **TNF-α** determination, the tissue was homogenized in lysis buffer containing protease inhibitor cocktail, the homogenates were centrifuged, at 12,000 g for 20 min at 4°C and the protein concentrations were determined by BCA protein assay. The levels of TNF-α were quantified with rat-specific ELISA kits according to the manufacturer's instructions (rat TNF-α from Diaclone, 865.000.096). Equal amounts of protein (35 μg per well) were used and each sample was assayed in duplicate. The TNF-α contents in the substantia nigra were obtained in picograms per millilitre of protein.

2.5 | ROCK activity assay

In animals of *Experiment I* and *Experiment II*, ROCK activity was measured with a ROCK Activity Assay Kit (CellBiolabs, Inc., San Diego, CA, USA) according to the manufacturer's instructions. The ROCK Activity Assay Kit is an enzyme immunoassay developed for detection of the specific phosphorylation of myosin phosphatase target subunit 1 at Thr696 by ROCK. Tissue was homogenized in lysis buffer (50-mM Tris–HCl pH 7.5, 150-mM NaCl, beta-glycerolphosphate 1mM, 1% Triton X-100, 1-mM EDTA, 1-mM EGTA, 1-mM Na_3VO_4) containing protease inhibitor cocktail (P8340, Sigma). Protein concentration of extracts was measured with the Pierce BCA Protein Assay Kit (Thermo Scientific) and equal amounts of protein (5 μg per well) were used; each sample was assayed in duplicate. Phosphorylation activity was assessed by measuring the absorbance at 450 nm in an Infinite M200 multiwell plate reader (TECAN).

2.6 | Real-time quantitative RT-PCR

Total RNA from the nigral region and striatum was extracted with the Trizol method according to the manufacturer's instructions. The RNA concentration was estimated using a NanoQuant plate and an Infinite M200 multiwell plate reader (TECAN, Salzburg, Austria). Total RNA (2 μg) was reverse-transcribed to cDNA with deoxynucleotide triphosphate (dNTP), random primers and Moloney murine leukaemia virus reverse transcriptase (M-MLV; 200 U, Invitrogen).

Real-time PCR was used to examine relative levels of *RhoA* mRNA and *ROCK II* mRNA. *β-actin* was used as housekeeping gene and was amplified in parallel with the genes of interest. Forward (F) and reverse (R) primers were designed for each gene by using NCBI Primer-BLAST (RRID:SCR_003095) (https://www.ncbi.nlm.nih.gov/tools/primer-blast); primers were located on the exon–exon junction to avoid amplification of genomic DNA. Primer sequences were as follows: for *RhoA*, forward 5′-GGACGGGAAGCAGGTAGAGTT-3′, reverse 5′-AACTATCA GGGCTGTCGATGGAA-3′; for *ROCK II*, forward 5′-GTTCAGTTGG TTCGTCATAAGGCA-3′, reverse 5′-TGAACCACCCACGGACTGTT-3′; and for *β-actin*, forward 5′-TCGTGCGTGACATTAAAGAG-3′, reverse 5′-TGCCACAGGATTCCATACC-3′. The standard curve of the different primers used in the study have the following efficiencies: 110% for *β-actin*, 110% for *RhoA* and 106% for *ROCK II*. Experiments were performed with a real-time iCyclerTM PCR platform (Bio-Rad, Hercules, CA, USA) using the IQ SYBR Green Supermix kit (Bio-Rad). The data were evaluated by the ΔΔCt method ($2^{-\Delta\Delta Ct}$) where Ct is the cycle threshold. The expression of each gene was obtained as relative to the housekeeping transcripts. The data were then normalized to the values of the control group and expressed as mean ± SEM.

2.7 | Immunohistochemistry

The animals used for immunohistochemistry were first perfused with 0.9% saline and then with cold 4% paraformaldehyde in 0.1-M phosphate buffer, pH 7.4. The brains were removed and subsequently washed and cryoprotected in the same buffer containing 20% sucrose and finally cut into 40-μm sections on a freezing microtome. The sections were incubated for 1 h in 10% normal swine serum with 0.25% Triton X-100 in 20-mM potassium PBS containing 1% BSA (KPBS-BSA) and then incubated overnight at 4°C with antibodies anti-TH as DA marker (mouse monoclonal anti-TH, Sigma-Aldrich Cat# T2928, RRID:AB_477569; 1:10,000). The sections were subsequently incubated, first for 60 min with the corresponding biotinylated secondary antibody (horse anti-mouse, Vector Laboratories Cat# BA-2001, RRID:AB_2336180; 1:200) and then for 90 min with avidin–biotin–peroxidase complex (ABC, 1:100, Vector). Finally, the labelling was revealed by treatment with 0.04% hydrogen peroxide and 0.05% 3,3′-diaminobenzidine (DAB, Sigma). In all experiments, control sections, in which the primary antibody was omitted, were immune-negative for TH.

2.8 | Data and analysis

The data and statistical analysis comply with the recommendations of the *British Journal of Pharmacology* on experimental design and analysis in pharmacology. All data were obtained from at least three independent experiments (i.e. not treating technical replicates as independent values) and expressed as means ± SEM. WB and PCR data were normalized to the values of the control group (100% or 1, respectively) and expressed as mean ± SEM. The rest of the data were presented as scores (behavioural data) or as absolute values (ELISA, pg·ml^{-1}). Statistical analysis was undertaken only for studies where each group size was at least n = 5, where n = number of independent values. Outliers were included in data analysis and presentation. The minimal number of animals per group has been estimated taking into account the principle of replacement, refinement and reduction (RRR), using the statistical calculator tool on the page https://www.imim.cat/ofertadeserveis/software-public/granmo/ of the Hospital Institute from the Sea of Medical Research of the Biomedical Research Park of Barcelona. Two-group comparisons were carried out by unpaired Student's *t*-test and multiple comparisons were analysed by one-way ANOVA followed by post hoc Holm–Sidak test. The post hoc tests were conducted only if F in ANOVA achieved $p < 0.05$ and there was no significant variance inhomogeneity. Dyskinetic behavioural data were analysed by two-way repeated measure (RM) ANOVA with treatment and time as factors followed by Holm–Sidak post hoc comparisons. The normality of populations and homogeneity of variances were analysed before each test. No approaches were used to reduce unwanted sources of variation by data normalization or to generate normal data. In a few cases of inhomogeneity, non-parametric tests of Mann–Whitney or Kruskal–Wallis were used to confirm statistical differences. Differences were considered statistically significant at $P < 0.05$ and the threshold value was not varied during the study. All statistical analyses were carried out with SigmaPlot 11.0 (RRID:SCR_003210) from Jandel Scientific, Systat Software, Inc., CA, USA.

2.9 | Nomenclature of targets and ligands

Key protein targets and ligands in this article are hyperlinked to corresponding entries in the IUPHAR/BPS Guide to PHARMACOLOGY http://www.guidetopharmacology.org are permanently archived in the Concise Guide to PHARMACOLOGY 2019/20 (Alexander et al., 2019).

3 | RESULTS

3.1 | Changes in RhoA/ROCK expression after dopaminergic denervation (6-OHDA lesion)

A first group of rats (Figure 2) was killed a week after the 6-OHDA injection to evaluate RhoA/ROCK expression after a short post-lesion period (i.e. during neuronal death and associated neuroinflammation). Consistent with our previous experiments in PD models (Rodriguez-Perez, Valenzuela, Villar-Cheda, Guerra, & Labandeira-Garcia, 2012; Rodriguez-Perez, Dominguez-Meijide, Lanciego, Guerra & Labandeira-Garcia, 2013; Villar-Cheda et al., 2012), we observed a significant increase of RhoA and ROCK protein levels and mRNA expression in the substantia nigra and striatum relative to control rats (Figure 2a–c). In the striatum and substantia nigra, we also studied levels of RhoA/ROCK when the 6-OHDA lesion was stabilized (4 weeks of 6-OHDA injection) and at the period (8 weeks post-lesion) in which 6-OHDA-lesioned rats can be compared with stable dyskinetic rats that have received 3 weeks of L-DOPA treatment. In these rats with long-term 6-OHDA lesions (i.e. 4 and 8 weeks after 6-OHDA injection; without additional treatments/ saline), we observed a significant decrease in RhoA/ROCK levels and ROCK activity relative to unlesioned controls (no change was detected in ROCK activity in the striatum at 8 weeks; Figure 2d–i). In summary, the increase in RhoA and ROCK protein/mRNA as a result of 6-OHDA lesion was only observed at the Week 1 time point and decreased in long-term lesions (see Section 4). The remaining lesioned animals were used to investigate the involvement of ROCK in development of L-DOPA-induced dyskinesia. Four weeks after lesion and before treatment with saline or L-DOPA, maximal dopaminergic lesions were confirmed (Figure 3). Analysis of the rotational behaviour (selected rats showed 893 ± 106 turns) and analysis of the forelimb akinesia in the cylinder test revealed maximal lesions (Figure 3a). The significant loss of TH immunoreactivity in the lesioned side was confirmed by western blot or immunohistochemistry at the end of the experiments (Figure 3b–d).

3.2 | Nigral and striatal RhoA/ROCK is increase in dyskinetic rats

A group of rats was daily injected with different doses of L-DOPA (6 or 12 mg·kg⁻¹; the range of doses used clinically) until consistent levels of AIMs were achieved (i.e. 3 weeks). As expected, the higher dose of L-DOPA resulted in more severe development of AIMs, which appeared earlier after injection. Integrated AIM score, calculated as the addition of limb, orolingual and axial components, reached values around 25% higher in animals injected with the 12 mg·kg⁻¹ of L-DOPA dose than in those injected with 6 mg·kg⁻¹. Rotation (i.e. locomotive movement) was also significantly higher in animals injected with 12 mg·kg⁻¹ of L-DOPA (about 65% higher). The time course of dyskinesia in animals treated with 12 mg·kg⁻¹ was around 2.5–3 h while in rats injected with 6 mg·kg⁻¹ was around 2 h (Figure 4).

Dyskinetic animals showed a significant increase (L-DOPA of 6 mg·kg⁻¹ and 12 mg·kg⁻¹) in the expression of RhoA and ROCK protein in the substantia nigra and striatum the latter only at 12 mg·kg⁻¹, as compared with lesioned rats not treated with L-DOPA (Figure 5a–d). Consistent with above described data on protein or mRNA expression, ROCK activity was significantly increased in the substantia nigra of dyskinetic rats relative to untreated 6-OHDA-lesioned rats or sham-operated rats not treated with L-DOPA. Interestingly, lesioned rats treated with L-DOPA that did not develop dyskinesia showed no significant increase in ROCK activity as compared with normal controls (Figure 5e). A significant increase in ROCK activity relative to normal controls was observed in the striatum of dyskinetic rats (even at the doses of 6 mg·kg⁻¹) (Figure 5g). The loss of TH (Figure 5f) and rotational behaviour (806 ± 80 turns in 90 min) in rats that did not develop dyskinesia were not different to those of dyskinetic rats (i.e. showed maximal lesions).

In order to know if a chronic L-DOPA treatment is necessary to induce the increase in RhoA/ROCK expression, an additional group of 6-OHDA-lesioned rats was injected with a single high dose of L-DOPA (12 mg·kg⁻¹) and killed 1 or 4 h after L-DOPA administration. These rats showed dyskinetic movements (although less intense than rats chronically treated with L-DOPA; see Figure 4, first time point) together with a marked significant increase in nigral and striatal *RhoA* and *ROCK* mRNA expression after L-DOPA injection in comparison with rats injected with vehicle (Figure 6a–d), both at 1 hand 4 h. The time course of a single L-DOPA injection (12 mg·kg⁻¹) is shown in Figure 6e,f.

3.3 | Fasudil reduces ROCK activity, inflammation and angiogenesis markers, and development of dyskinesia

Treatment of dyskinetic rats with fasudil (10 or 40 mg·kg⁻¹·day⁻¹) induced a significant decrease in ROCK activity both in the nigra and the striatum (Figure 5e,g). Injection of L-DOPA (i.e. in dyskinetic rats) induced a significant increase in angiogenesis-related markers such as VEGF relative to non-lesioned controls and untreated 6-OHDA-lesioned rats and inflammation-related markers such as IL-1β and TNF-α relative to non-lesioned controls and untreated 6-OHDA-lesioned rats (Figure 7). Treatment with fasudil (10 and 40 mg·kg⁻¹) significantly decreased the effect of L-DOPA on levels of VEGF, TNF-α and IL-1β.
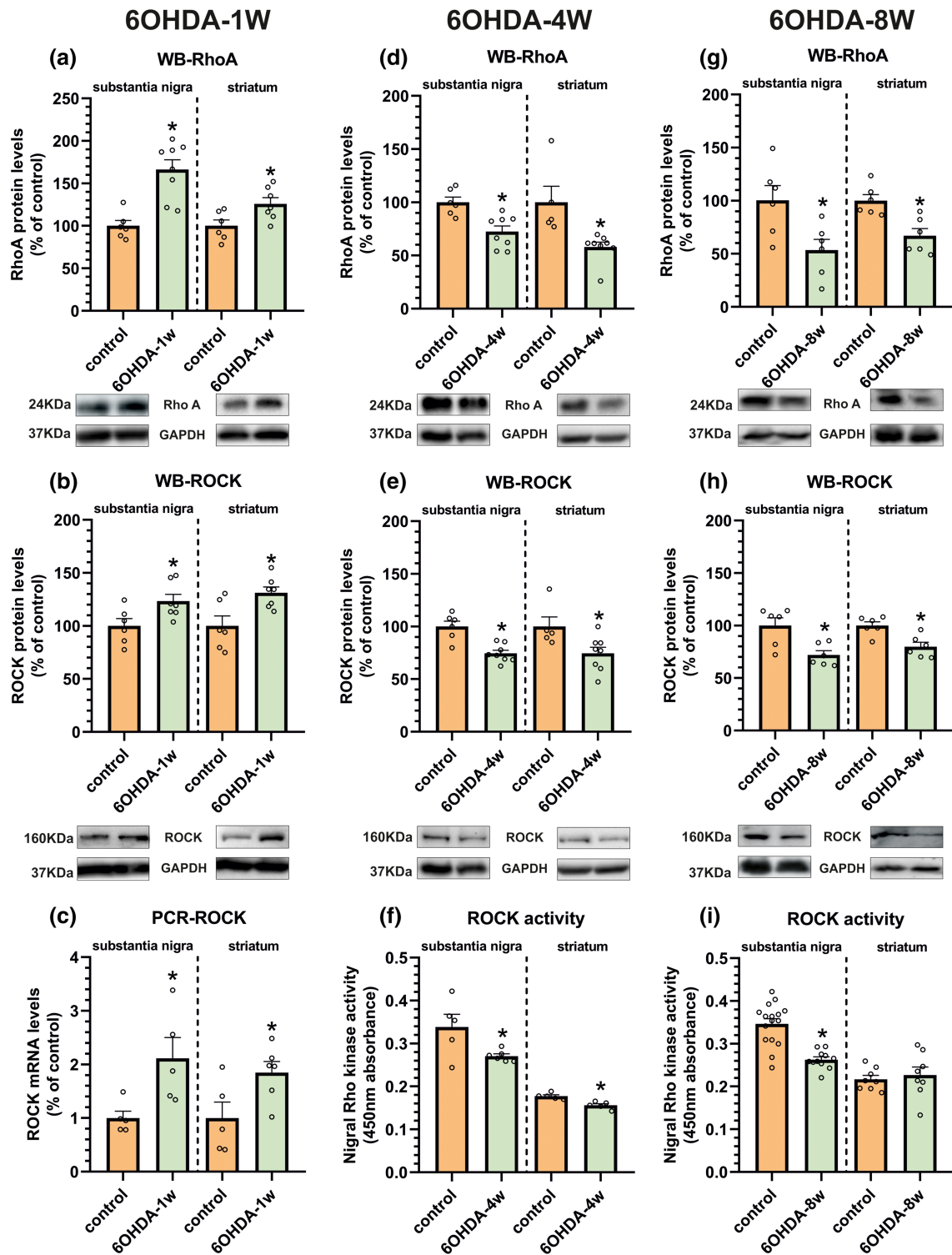
FIGURE 2 Effect of short-term (1 week) and long-term (4 and 8 weeks) 6-OHDA lesions on the RhoA/ROCK pathway in the striatum and substantia nigra relative to non-denervated (i.e. sham-operated) controls. Short-term dopaminergic denervation induced a significant increase in the expression of RhoA and ROCK protein levels determined by western blot (WB; a, b) and mRNA levels analysed by RT-PCR (c). In long-term lesions, RhoA and ROCK protein levels were decreased (d, e, g, h). ROCK activity assays (f, i) confirmed a decreased ROCK activity in the nigra and 4-week-lesioned striatum (not significant at 8 weeks). Protein expression was determined relative to the GAPDH band value and the expression of each gene was determined relative to the housekeeping transcripts (β-actin). The results were normalized to the values for non-lesioned control rats. Data are means ± SEM. *$P < 0.05$ (unpaired Student's t-test)
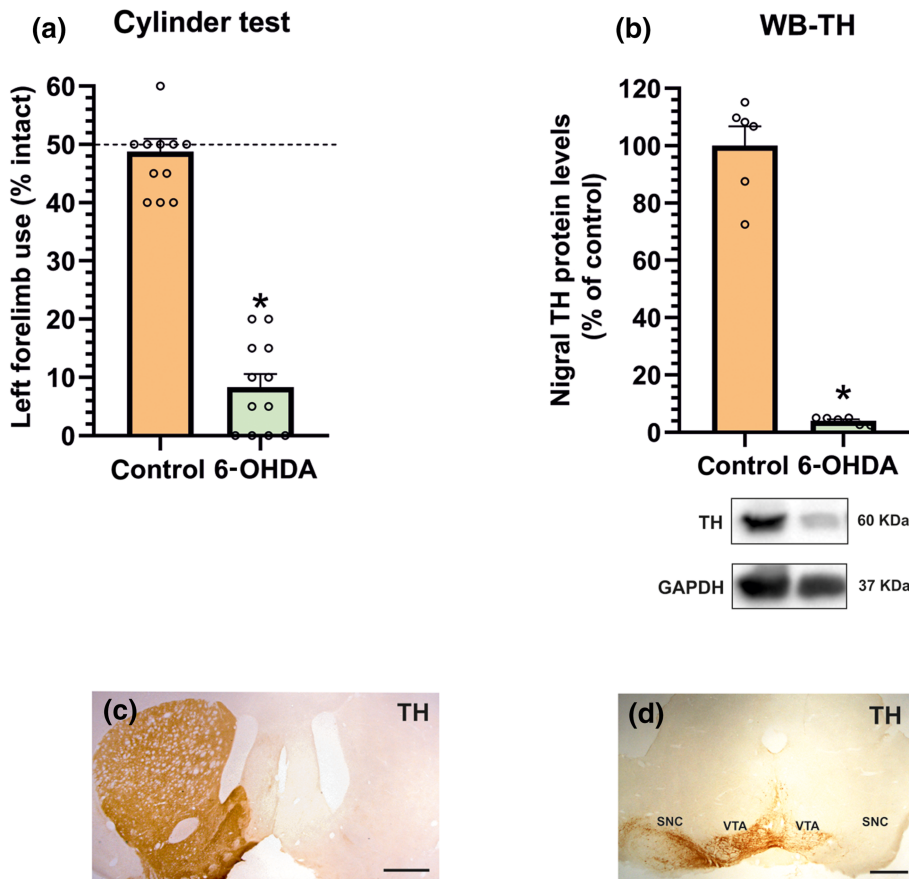
FIGURE 3 Rats with chronic dopamine denervation showed a marked reduction in the left forelimb use relative to non-denervated controls, as assessed by cylinder test (a) and intense amphetamine-induced rotational behaviour (893 ± 106 turns in 90 min). The maximal lesion (i.e. lack of tyrosine hydroxylase (TH) expression) was confirmed at the end of the experiments by western blot (WB) analysis (b) or immunohistochemistry in the striatum (c) and substantia nigra (d). WB results were normalized to the values of the non-lesioned control rats. Data are means ± SEM. *P < 0.05 (unpaired Student's t-test). SNC, substantia nigra compacta; VTA, ventral tegmental area. Scale bars: 500 μm

Consistent with the involvement of ROCK overactivation in L-DOPA-induced dyskinesia, rats treated with 10 mg·kg⁻¹ of fasudil and L-DOPA showed a significant reduction in dyskinesia relative to rats treated with L-DOPA alone. The significant differences in integrated AIM score were observed from the fifth day of treatment until the end of the 3-week evaluation period (Figure 8a; see also AUC representations in Figure 8). ROCK inhibition by fasudil produced a significant reduction in L-DOPA-induced dyskinesia in the different components (Figure 8c–g): limb component (around 20% decrease), axial component (around 30% decrease) and orolingual component (around 25% decrease). Animals injected with 40 mg·kg⁻¹ of fasudil showed higher significant decrease (around 50% decrease) in the dyskinesia scores (Figure 8b). The decrease in L-DOPA-induced dyskinesia was observed in all components analysed (Figure 8d,f,h). This reduction was observed from the fifth L-DOPA injection until the end of the evaluation period. At the end of the 3-week period of treatment (i.e. on the ninth week after 6-OHDA injection), the L-DOPA dose was increased (24 mg·kg⁻¹) to investigate whether fasudil was also effective against more severe dyskinesia. Fasudil also reduced significantly the higher dyskinetic behaviour induced by 24 mg·kg⁻¹ of L-DOPA (Figure 8b). The decrease in L-DOPA-induced dyskinesia induced by 24 mg·kg⁻¹ of L-DOPA was observed in all components analysed (Figure 8d,f,h).

We performed the stepping test and the cylinder test to investigate the impact of the ROCK inhibitor fasudil on the therapeutic effect of L-DOPA. Both in the stepping and cylinder tests,

administration of L-DOPA induced (90 min after injection) a marked significant improvement of left paw use relative to baseline scores and 6-OHDA-lesioned rats injected with saline). Animals treated with L-DOPA alone were not significantly different from those treated with L-DOPA and fasudil (10 or 40 mg·kg⁻¹), which revealed that the therapeutic effect of L-DOPA was preserved relative to baseline and 6-OHDA-lesioned rats injected with saline (Figure 9a,b). In addition, L-DOPA-induced rotation/locomotive movement was also unaffected by fasudil administration, showing that the observed decrease in L-DOPA-induced dyskinesia was not a consequence of a fasudil-induced reduction in motor activation (Figure 9c). Note that the cylinder, stepping and rotometer (less affected by dyskinesia) tests were performed after the second, fourth and sixth L-DOPA injection, respectively, to prevent any possible interference of the dyskinesias, which began to be significant after the fifth injection, with behavioural test performance.

3.4 | Effect of fasudil on previously established dyskinetic behaviour

An additional group of 6-OHDA-lesioned rats (Experiment IV) was primed with daily injections of L-DOPA for 3 weeks (i.e. until L-DOPA-induced dyskinesia were consistently stable) and then rats were treated with L-DOPA and fasudil in order to investigate whether ROCK inhibition could reduce AIMs once dyskinesia was established.
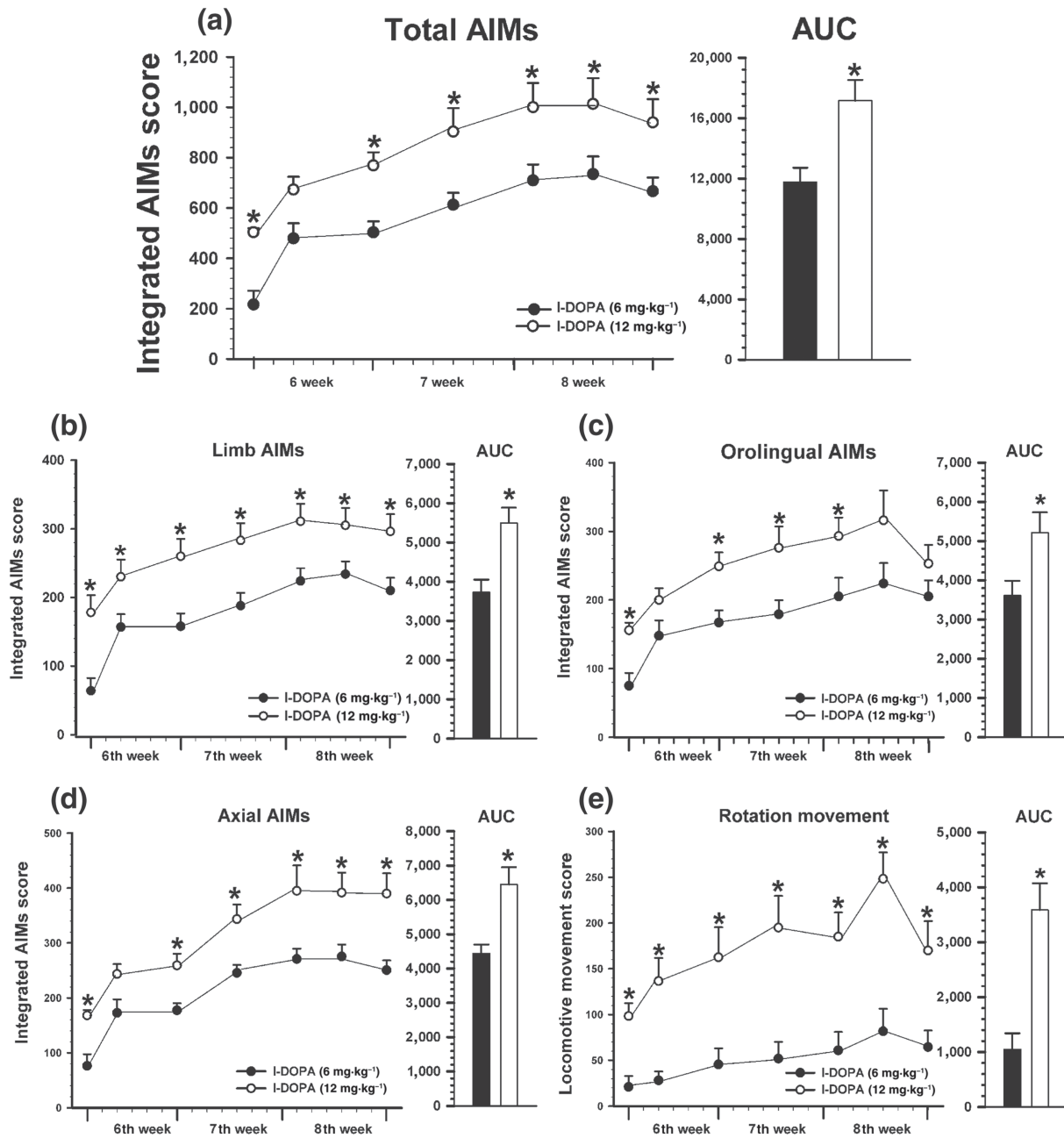
FIGURE 4 Development of dyskinesia induced by chronic L-DOPA treatment (21 days; sixth, seventh and eighth week) at high (12 mg·kg^{-1}, white circles; $n = 6$) and low (6 mg·kg^{-1}, black circles; $n = 11$) doses. Total AIM score (a) was estimated as the addition of limb (b), orolingual (c) and axial (d) components. Rotational movement was recorded as locomotive component (e). Data are means ± SEM. *$P < 0.05$ (unpaired Student's t test for each time point). Student's t-test (AUC) and two-way ANOVA for repeated measures and Holm–Sidak post hoc test. AIMs, abnormal involuntary movements

Using 10 mg·kg^{-1}·day^{-1} of fasudil, the animals did not show any significant reduction on AIM scores, even after prolonging fasudil treatment for an additional week or increasing L-DOPA dose up to 24 mg·kg^{-1} (Figure 10a,b). However, a higher dose of fasudil (40 mg·kg^{-1}) produced a significant reduction of dyskinesia from the third day of fasudil treatment (around 40% decrease; Figure 10c,d). This reduction was also observed in the different components analysed (Figure 10e–h). Interestingly, when we increased the L-DOPA dose to 24 mg·kg^{-1} (on the 10th week after 6-OHDA

injection), the L-DOPA-induced dyskinesia reduction was even higher and this reduction continued until we finished the treatment period (45%, reduction in the last injection; Figure 10d).

4 | DISCUSSION

In several PD models, ROCK inhibitors such Y27632 or fasudil have shown neuroprotective properties for dopaminergic neurons through
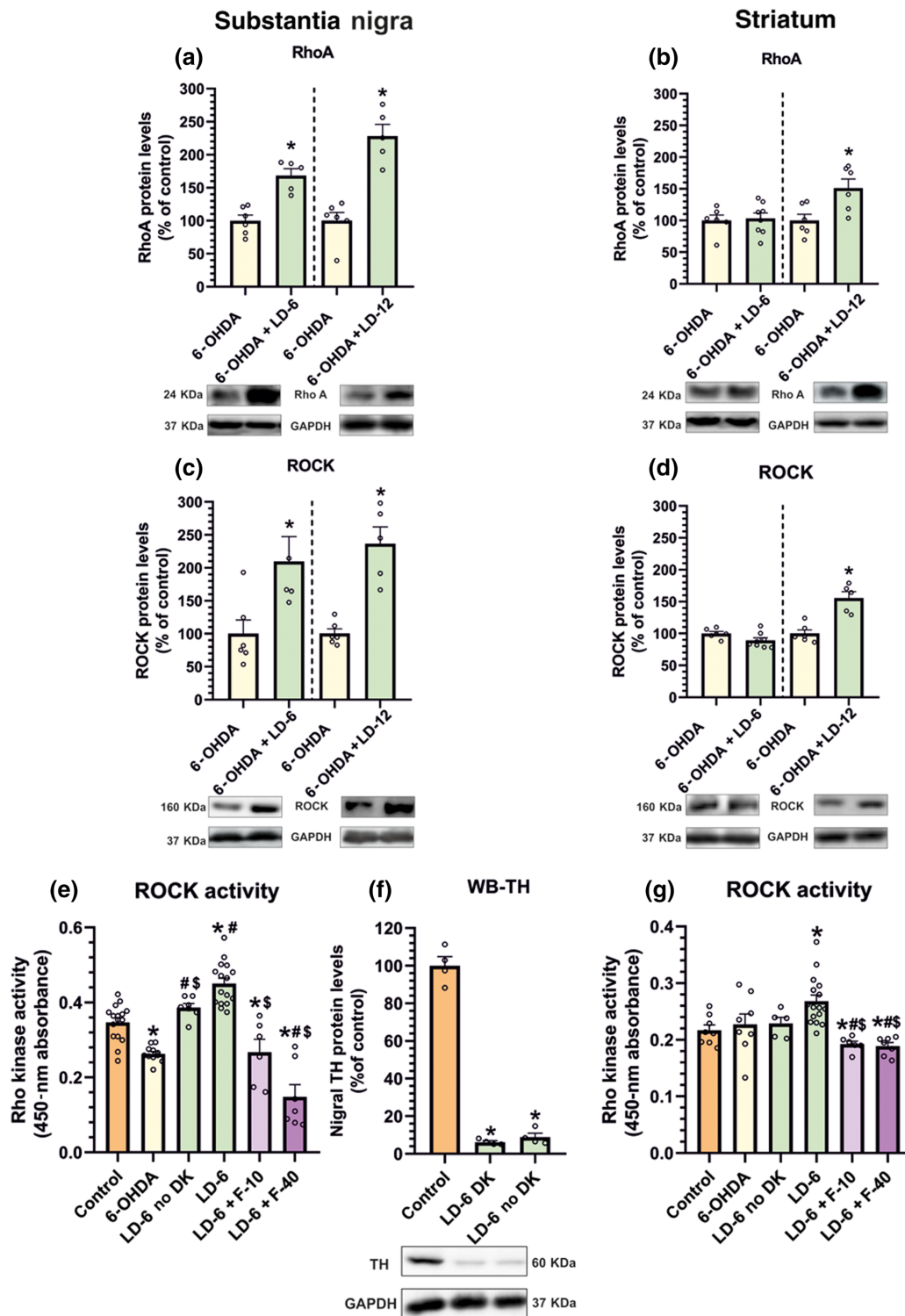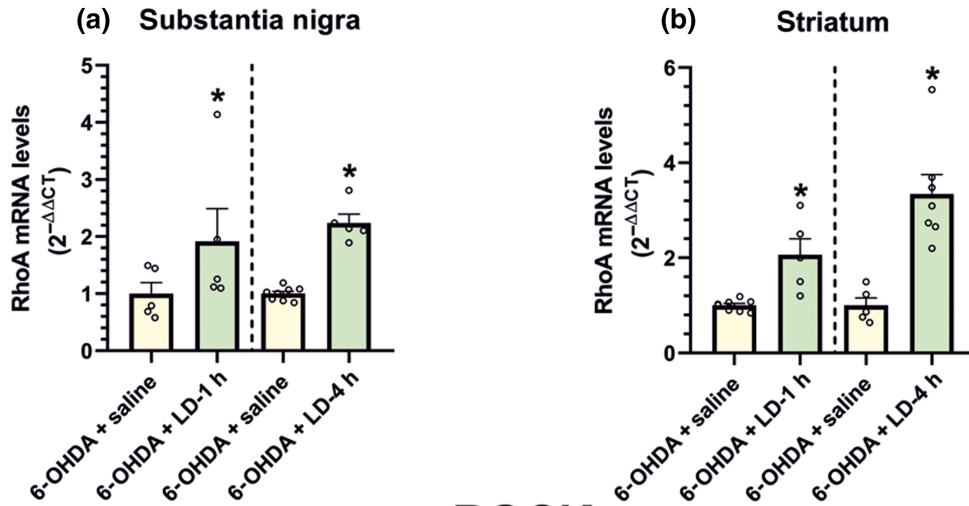
FIGURE 5 RhoA (a, b) and ROCK (c, d) protein levels in the substantia nigra and striatum of 6-OHDA rats chronically treated with saline and dyskinetic rats chronically treated with L-DOPA (6 mg·kg^{-1}, LD-6; or 12 mg·kg^{-1}, LD-12). (e–g) ROCK activity in untreated controls, untreated 6-OHDA-lesioned rats and 6-OHDA-lesioned rats treated with L-DOPA (6 mg·kg^{-1}·day^{-1}) that developed or did not develop dyskinesia (DK). Dyskinetic rats showed a significant increase in ROCK activity relative to saline-injected lesioned rats and non-lesioned controls. Interestingly, no significant increase relative to unlesioned controls was observed in L-DOPA-treated rats that did not develop dyskinesia. Treatment with fasudil (10 or 40 mg·kg^{-1}; F-10, F-40) induced a marked decrease in ROCK activity both in the nigra and in the striatum (e, g). WB for TH (f) and rotational behaviour showed same levels of dopaminergic denervation in dyskinetic and non-dyskinetic rats. In (a)–(d), the results were normalized to the values of 6-OHDA-lesioned animals treated with saline and data are means ± SEM. *$P < 0.05$ (unpaired Student's t-test). In (e)–(g), one-way ANOVA and Holm–Sidak post hoc test were used (*$P < 0.05$, significant differences relative to controls; #$P < 0.05$, significant differences relative to 6-OHDA; $P < 0.05$, significant differences relative to L-DOPA)
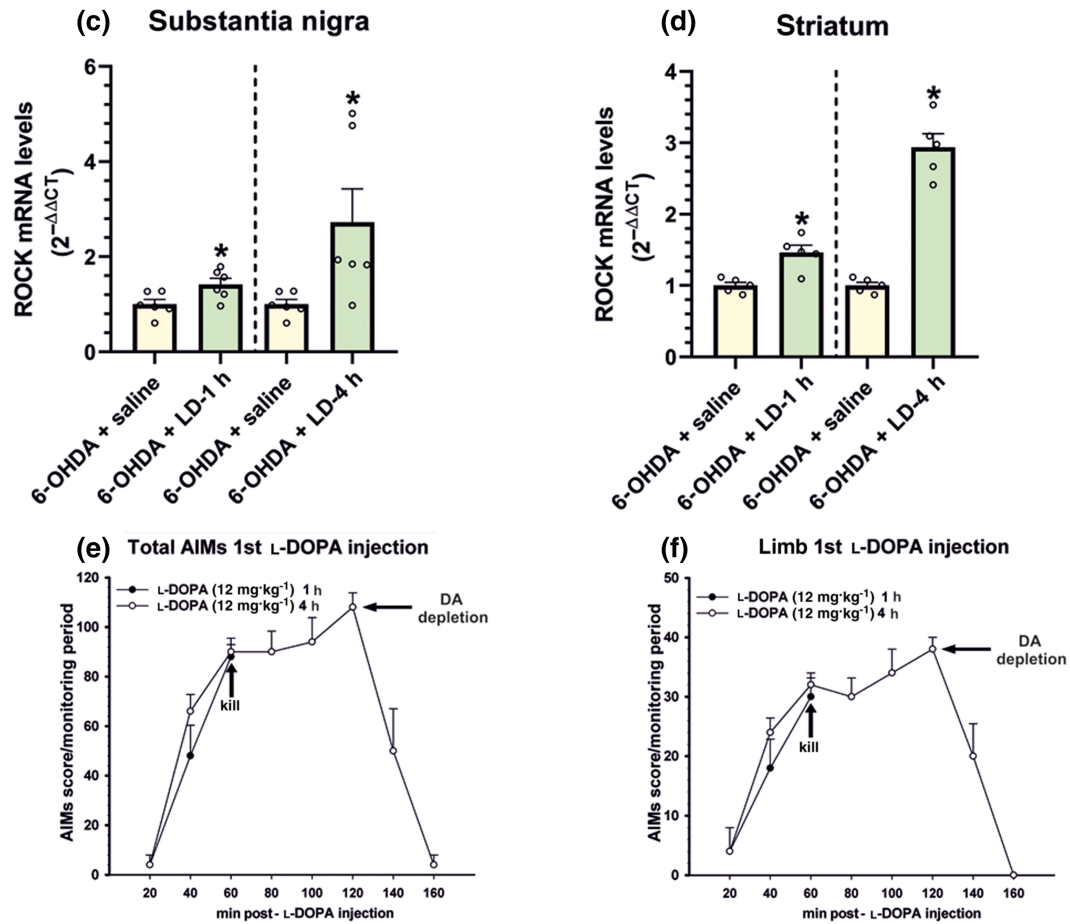
RhoA

ROCK

FIGURE 6 Effect of acute L-DOPA treatment on RhoA and ROCK mRNA levels. A single injection of a high dose of L-DOPA (LD; 12 mg·kg^{-1}) induced dyskinesia and a significant increase in RhoA (a, b) and ROCK (c, d) mRNA levels in the substantia nigra (a, c) and striatum (b, d). In (a)–(d), the results were normalized to the values of 6-OHDA-lesioned rats treated with saline. Time course of total AIMs (e) and the limb component (f) in rats subjected to a single L-DOPA injection and killed 1 h (n = 5) and 4 h (n = 5) after injection. Data are means ± SEM. *P < 0.05 (Student's t test)
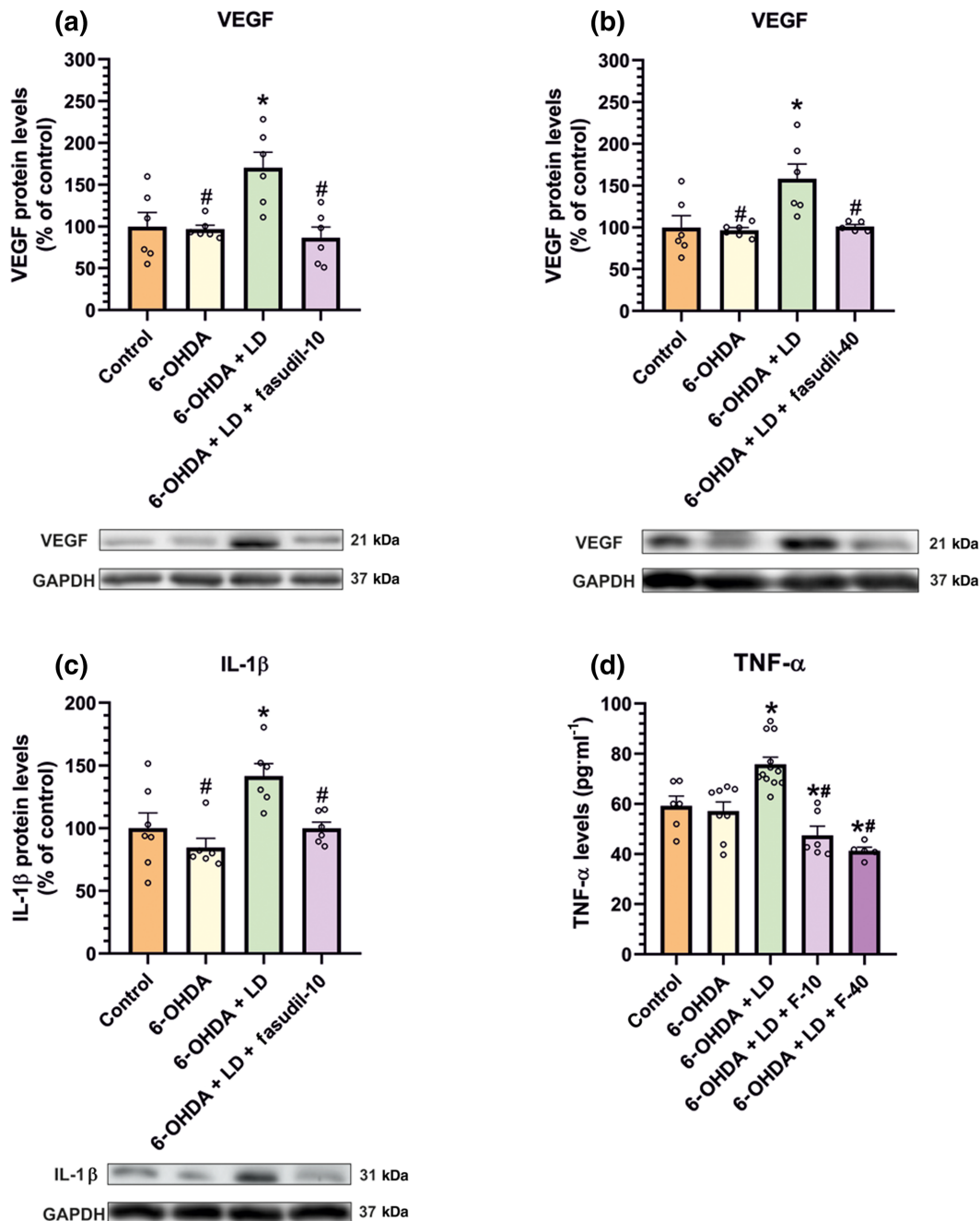
FIGURE 7 Effect of fasudil (10 or 40 mg·kg^{-1}; F-10, F-40) compared to non-lesioned controls and untreated 6-OHDA-lesioned rats on markers related to angiogenesis and neuroinflammation in the substantia nigra. Protein levels of the angiogenesis-related factor VEGF (a, b) and the pro-inflammatory markers IL-1β (c) and TNF-α (d) were increased in rats subjected to L-DOPA treatment and significantly decreased in rats treated with L-DOPA (6 mg·kg^{-1}) and fasudil, as determined by WB (a–c) and ELISA analysis (d). The results were normalized to the values of non-lesioned controls. Data are means ± SEM. *$P < 0.05$, significant difference relative to controls; #$P < 0.05$, significant difference relative to L-DOPA-treated animals (one-way ANOVA and Holm–Sidak post hoc test)

several mechanisms (Barcia et al., 2012; Moskal et al., 2020; Tatenhorst et al., 2014; Villar-Cheda et al., 2012). For the first time, the present results show that inhibition of ROCK activity with fasudil significantly reduces development of L-DOPA-induced dyskinesia (Figure 8). Moreover, fasudil was effective in reducing already established L-DOPA-induced dyskinesia (Figure 10). A low dose (10 mg·kg^{-1}), which was effective in neuroprotective studies (Rodriguez-Perez et al., 2015; Wu et al., 2012), showed significant

effects against L-DOPA-induced dyskinesia development but had no effect on rats with already developed L-DOPA-induced dyskinesia. However, higher doses (40 mg·kg^{-1}) led to significant reduction of already established dyskinesia. This dose was also effective against high levels of dyskinesia induced by 24 mg·kg^{-1} of L-DOPA, even in rats that had developed dyskinesia previous to treatment with fasudil (Figures 8 and 10). The efficiency of fasudil in reducing dyskinesia in both scenarios (i.e. reduction of development of dyskinesias in rats
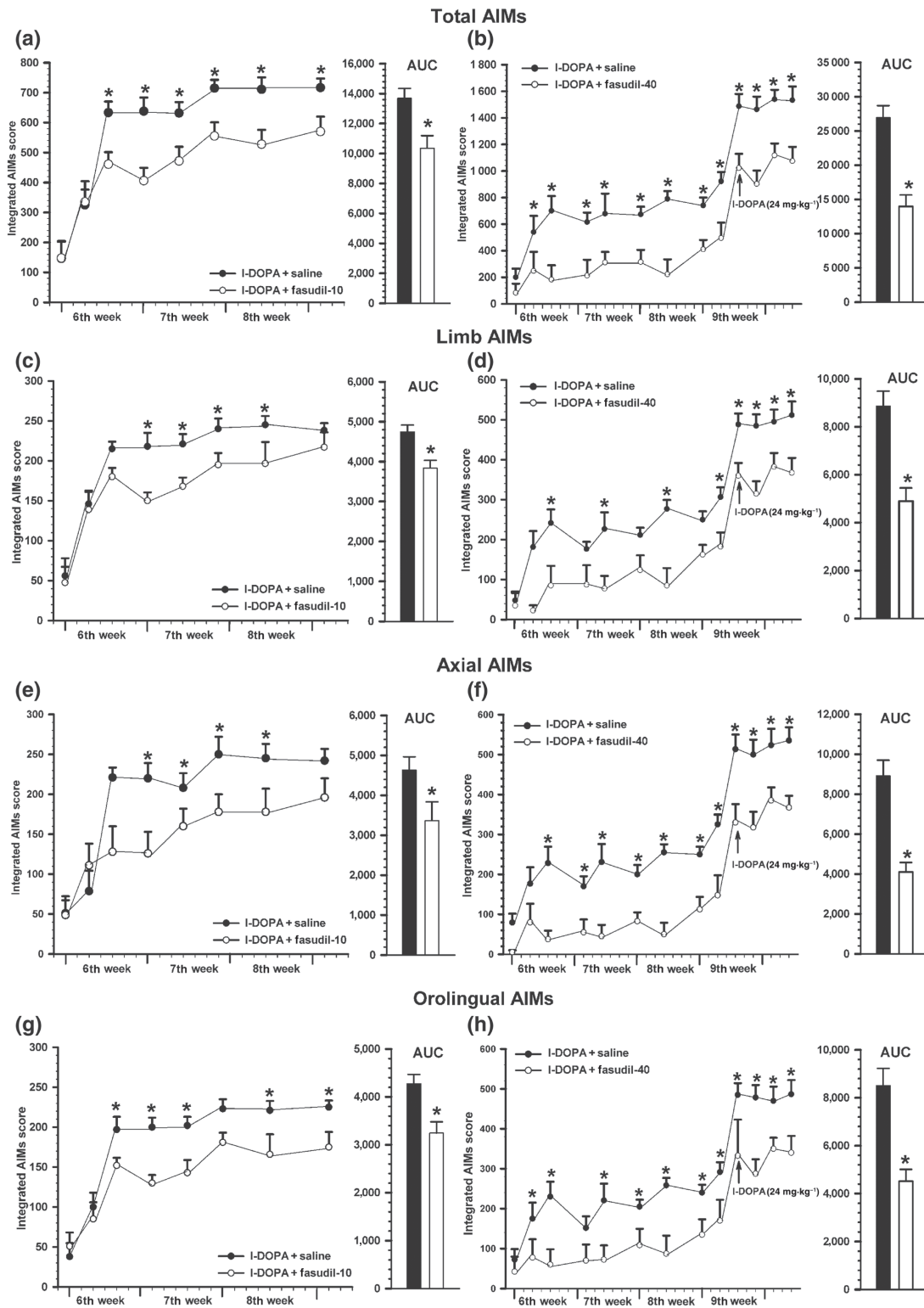
Total AIMs

FIGURE 8 Effect of fasudil on the development of L-DOPA-induced dyskinesia. Rats treated for 3 weeks (sixth, seventh and eighth) with L-DOPA (6 mg·kg^{-1}) + saline or L-DOPA + 10 mg·kg^{-1} fasudil (n = 8 in both groups; a, c, e, g) and rats treated with L-DOPA (6 mg·kg^{-1}) + saline or L-DOPA + 40 mg·kg^{-1} fasudil (n = 6 in both groups; b, d, f, h) revealed a significant reduction in the severity dyskinesia in rats treated with L-DOPA + fasudil (white circles) relative to rats treated with L-DOPA + saline (black circles). A significant decrease was observed in the AIMs total score (a, b) and in the different components: limb (c, d), axial (e, f) and orolingual (g, h) dyskinesias. On the ninth week (fourth week of treatment, arrow), the dose of L-DOPA was increased to 24 mg·kg^{-1} to increase level of dyskinesia, which was significantly reduced by fasudil at 40 mg·kg^{-1} (b, d, f, h). Note that there are differences in y-axis scale in different panels (right and left panels and total AIMs relative to AIM components). The AUCs are also shown in (a)–(h). Data are means ± SEM. *P < 0.05. unpaired Student's t-test (AUC), and two-way ANOVA for repeated measures and Holm–Sidak post hoc test. AIMs, abnormal involuntary movements
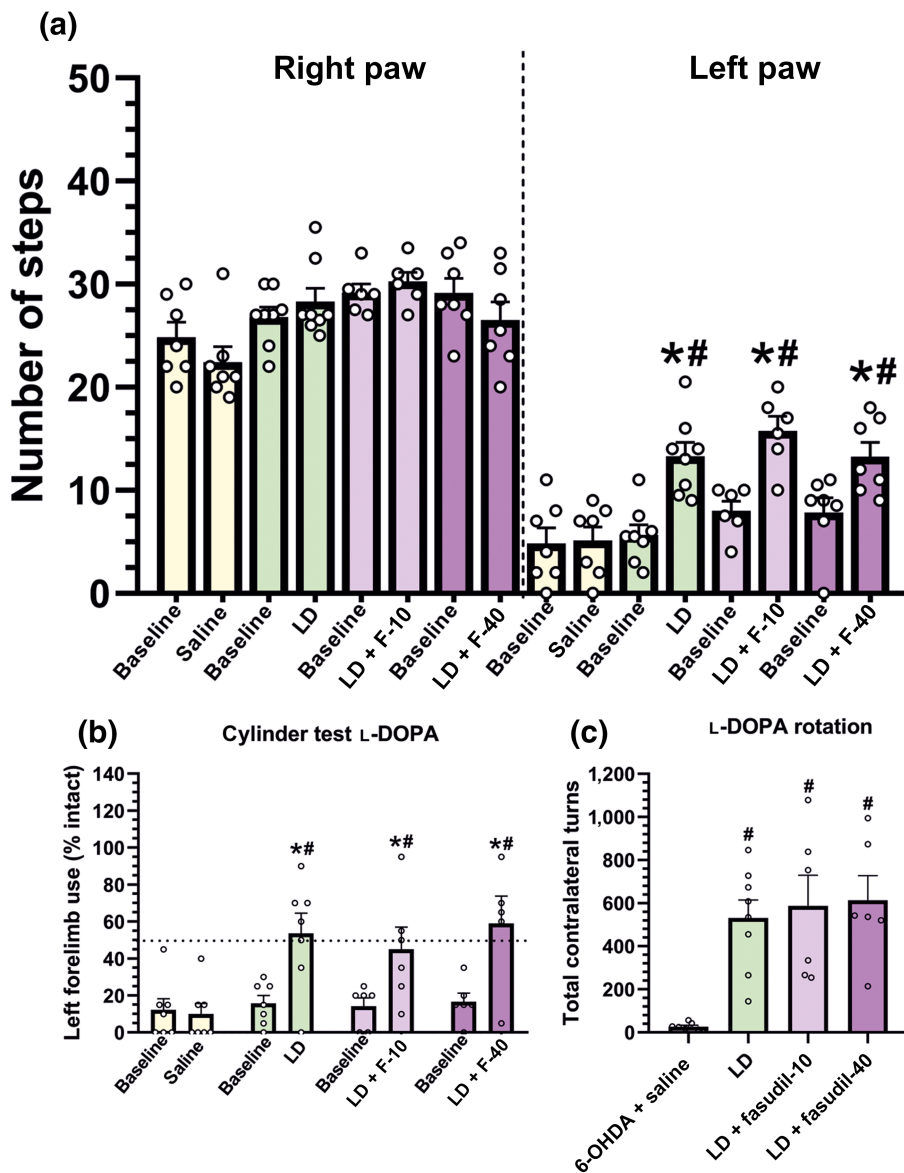
FIGURE 9 Effect of fasudil (10 and 40 mg·kg^{-1}; F-10, F-40) on the therapeutic effect of L-DOPA (LD; 6 mg·kg^{-1}·day^{-1}), which was assessed by the stepping test (a), spontaneous forelimb use in the cylinder test (b) and turning behaviour (c). Motor behaviour of 6-OHDA-lesioned rats before L-DOPA injection (baseline), or injected with saline instead of L-DOPA, or injected with L-DOPA alone, or injected with L-DOPA + fasudil was analysed. Administration of fasudil did not reduce the ability of L-DOPA to improve forelimb akinesia (a, b) or to induce contralateral rotational behaviour (c). Data are means ± SEM (*$P < 0.05$, significant differences relative to baseline levels, off L-DOPA, unpaired Student's t-test; #$P < 0.05$, significant differences relative to 6-OHDA-lesioned rats injected with saline)

previously treated with fasudil and reduction of dyskinesia in rats with already developed L-DOPA-induced dyskinesia) suggests that fasudil may be used for neuroprotection in patients without L-DOPA-induced dyskinesia and to delay and reduce development of L-DOPA-induced dyskinesia, and may be also effective for treating PD patients with already developed L-DOPA-induced dyskinesia. We also investigated the possibility that the reduction in dyskinesia may be related to the reduction of L-DOPA motor activity (Figure 9). However, several behavioural tests showed that fasudil decreased L-DOPA-induced dyskinesia without affecting the motor response to L-DOPA.

Fasudil and its analogues have been shown to inhibit ROCK activity and be effective against several diseases and disease models (Chen et al., 2013; Defert & Boland, 2017). In the present study, we observed that short-term 6-OHDA lesions (i.e. 1 week post-lesion) showed an increase in the expression of RhoA/ROCK in the substantia nigra and striatum, which is consistent with the increase in ROCK activity that mediates the neuroinflammation during the neurodegenerative process (Barcia et al., 2012; Borrajo, Rodriguez-

Perez, Villar-Cheda, Guerra, & Labandeira-Garcia, 2014; Villar-Cheda et al., 2012). Rats with long-term 6-OHDA lesions showed a decrease in protein expression and ROCK activity relative to short-term lesions, which is consistent with several time course studies on nigrostriatal neurodegeneration showing a time-related decrease in neuroinflammatory markers after neurotoxic lesions (Walsh, Finn, & Dowd, 2011). A decrease below control levels may be related to the important loss of dopaminergic neurons and/or denervation-related compensatory changes resulting in lower levels of RhoA/ROCK (Koch et al., 2018; Labandeira-Garcia et al., 2015). Neuroinflammation plays a major role in the progression of PD (Gerhard et al., 2006). In contrast with that observed in long-term 6-OHDA lesions, in which the neurodegenerative process is completed, post-mortem brain sections of PD patients showed increased ROCK expression in astrocytes and microglia, suggesting an active neuroinflammatory process (Koch et al., 2018). Therefore, in PD reduction of ROCK activity by fasudil may have more efficient neuroprotective and antidyskinetic effects.
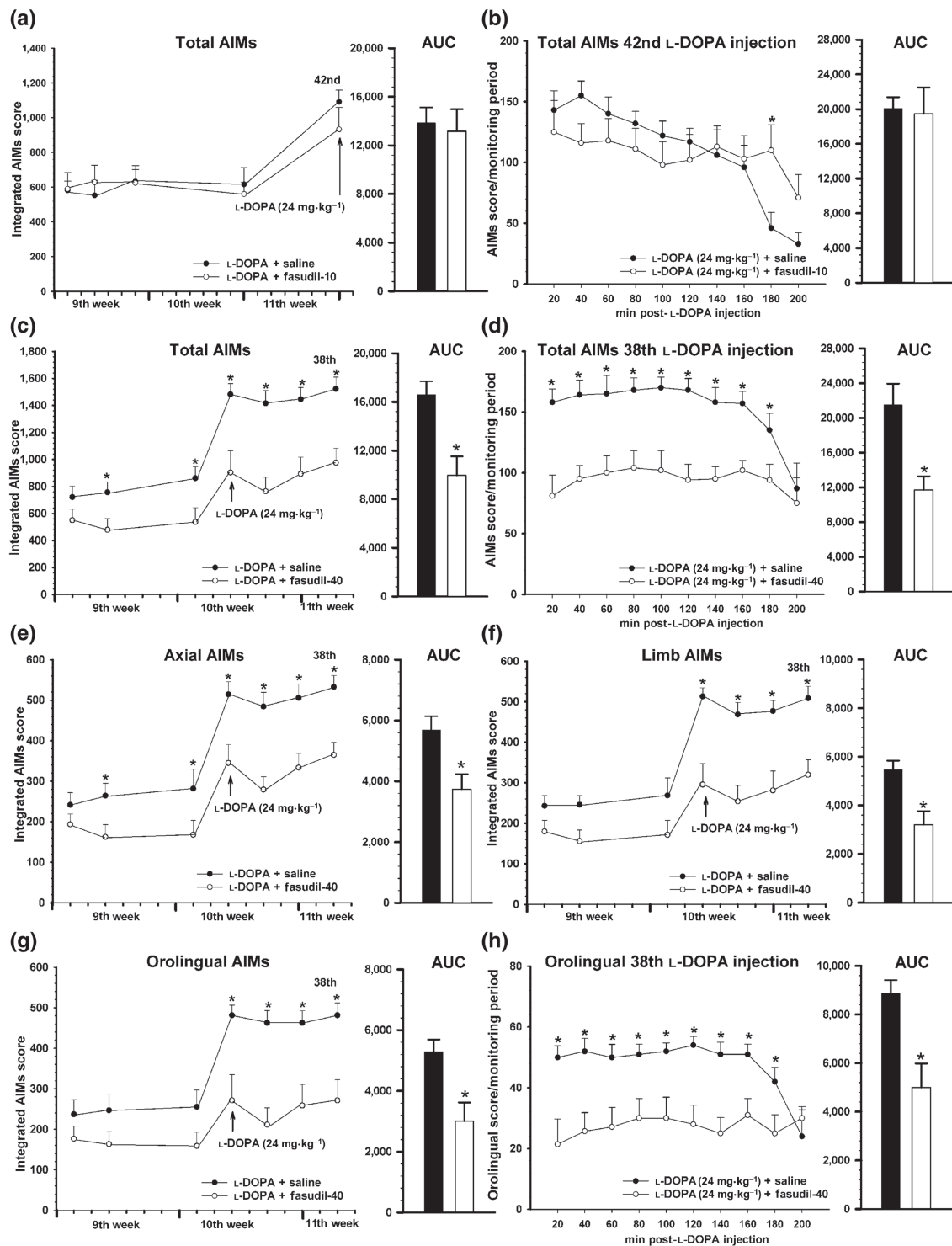
FIGURE 10 Effect of fasudil in rats with previously established L-DOPA-induced dyskinesia (LID) and showed as integrated AIMs (a, c, e–g) and time course of a single injection (b, d, h). Rats ($n = 34$) were treated with L-DOPA only (6 mg·kg^{-1}) for 3 weeks (sixth to eighth week; i.e. until LID were consistently established). Then (9th to 11th week) rats received L-DOPA (6 mg·kg^{-1}) + saline (black circles) or L-DOPA + fasudil (10 or 40 mg·kg^{-1}; white circles). Treatment with 10 mg·kg^{-1} of fasudil ($n = 9$) did not produce any significant effect on the dyskinetic behaviour relative to rats treated with L-DOPA + saline ($n = 9$), even when treatment was prolonged up to the 42nd injection or the L-DOPA dose was increased to 24 mg·kg^{-1} (arrow; a). The time course (200 min) of AIMs in the last injection (42nd injection; 24 mg·kg^{-1}) is shown in (b). However, treatment with 40 mg·kg^{-1} of fasudil ($n = 8$) induced a significant reduction in LID relative to animals treated with L-DOPA + saline ($n = 8$), including that produced by injection of high doses (24 mg·kg^{-1}; arrow) of L-DOPA (c–h). The decrease was observed in the AIMs total score (c, d) and in the different components analysed: axial (e), limb (f) and orolingual (g, h). The time course of AIMs (d) and orolingual component (h) of the last L-DOPA injection of this experiment (38th injection; 24 mg·kg^{-1}) is also shown. Data are means ± SEM. *$P < 0.05$. unpaired Student's t-test (AUC) and two-way ANOVA for repeated measures and Holm–Sidak post hoc test. AIMs, abnormal involuntary movements; LID, levodopa-induced dyskinesia

In dyskinetic rats, chronic L-DOPA injection again increased levels of RhoA/ROCK and pro-inflammatory markers, which were inhibited by treatment with fasudil, together with the reduction in the dyskinetic behaviour. Moreover, in rats with maximal dopaminergic denervation, a single injection of L-DOPA induced dyskinetic behaviour and increased RhoA/ROCK levels, although levels of dyskinesia further increased after several L-DOPA injections. Interestingly, a few denervated rats treated with L-DOPA did not develop dyskinesia and did not show the increase in ROCK activity observed in dyskinetic rats. This suggests that the increase in ROCK activity is associated to the dyskinetic behaviour and not just to L-DOPA administration. We consider that these non-dyskinetic rats were not the result of an incomplete dopaminergic lesion, because they were selected with the same criterion for maximal lesion than other rats, showed a similar lack of TH immunoreactivity in post-mortem analysis and these resistant rats were also found in many other studies (Carta et al., 2006; Ohlin et al., 2012). In any case, this result shows association between absence of increased levels of ROCK activity and absence of L-DOPA-induced dyskinesia.

The effect of ROCK on development of L-DOPA-induced dyskinesia may be due to the major role of ROCK in several mechanisms that are involved in development of L-DOPA-induced dyskinesia, particularly neuroinflammation and abnormal angiogenesis. Previous studies have shown that neuroinflammation is involved in the pathophysiology of L-DOPA-induced dyskinesia. Increased levels of IL-1β (Barnum et al., 2008; Muñoz et al., 2014) and other markers of inflammation were observed in the nigra and striatum of dyskinetic animals (Mulas et al., 2016) in the present and previous studies. L-DOPA-induced dyskinesia was increased by inflammatory insults such as LPS (Mulas et al., 2016; Pisanu et al., 2018). Anti-inflammatory drugs, such as ibuprofen (Teema et al., 2016), or immunomodulatory drugs, such as thalidomide (Boi et al., 2019), delayed the development of dyskinesia. Other strategies against L-DOPA-induced dyskinesia such as NOS inhibitors also inhibited neuroinflammation (Bortolanza et al., 2015; Padovan-Neto et al., 2015). Activation of microglial ROCK mediates several major components of the neuroinflammatory response such as microglial migration and phagocytosis, NADPH-oxidase activation and release of pro-inflammatory cytokines such as TNF-α (Borrajo, Rodriguez-Perez, Diaz-Ruiz, Guerra, & Labandeira-Garcia, 2014; Labandeira-Garcia et al., 2015; Rodriguez-Perez et al., 2015). In the present study, we confirmed that fasudil decreased the levels of the inflammatory markers, which were increased in dyskinetic rats. Furthermore, ROCK regulates transendothelial migration and infiltration of peripheral immune cells into the CNS (Heasman & Ridley, 2010; Honing et al., 2004). A number of mechanisms may link neuroinflammation and the development of dyskinesia. Neuroinflammation-related cytokines are involved in neurotransmitter synthesis and metabolism, brain plasticity and modulation of synaptic strength (Beattie et al., 2002). Effects of cytokines on glutamate appear particularly relevant (Takeuchi et al., 2006). Consistent with this, the glutamate NMDA receptor antagonist amantadine is currently used as a treatment for L-DOPA-induced dyskinesia, although long-term use of this compound causes complications

(Espay et al., 2018). In addition to the effects on glutamate, ROCK activation and inflammation-related compounds may modulate other neurotransmitters involved in dyskinesia such as dopamine (Sakai, Kaufman, & Milstien, 1995) and 5-hydroxytryptamine (Muñoz et al., 2008; Wu, Dissing-Olesen, MacVicar, & Stevens, 2015). Direct interactions between ROCK and 5-hydroxytryptamine have also been observed (Mair, MacLean, Morecroft, Dempsie, & Palmer, 2008).

L-DOPA-induced dysregulation of angiogenesis is also involved in L-DOPA-induced dyskinesia. Several studies showed altered BBB transport and up-regulation of angiogenic markers after chronic L-DOPA treatment in rats (Lerner et al., 2017; Ohlin et al., 2011) and humans (Ohlin et al., 2011). Dyskinetic animals and patients showed increased levels of VEGF and the VEGF inhibitor vandetanib attenuates the development of dyskinesias (Ohlin et al., 2011). Altered BBB properties associated to an accelerated angiogenesis may lead to uncontrolled L-DOPA delivery, glial activation and neuroinflammation, which contribute to the development of L-DOPA-induced dyskinesia.

ROCK inhibition may also reduce L-DOPA-induced dyskinesia through inhibition of angiogenesis. RhoA/ROCK signalling is essential for multiple aspects of VEGF-mediated angiogenesis (Bryan et al., 2010; Sun, Breslin, Zhu, Yuan, & Wu, 2006), including endothelial cell survival, differentiation and migration, and BBB permeability (Hoang, Whelan, & Senger, 2004). Consistent with this, inhibition of ROCK pathway blocked angiogenesis (Bryan et al., 2010), as well as VEGF-induced microvascular endothelial hyperpermeability (Sun et al., 2006) and fasudil suppressed glioma-induced angiogenesis by targeting ROCK and ERK (Nakabayashi & Shimizu, 2011). In the present study, we observed that fasudil decreases VEGF levels together with ROCK activity and dyskinesia in L-DOPA-treated rats.

Interestingly, several drugs acting against L-DOPA-induced dyskinesia may converge on the regulation of RhoA/ROCK activity. Angiotensin AT$_1$ receptor antagonists (Muñoz et al., 2014; Rodriguez-Perez et al., 2012) may reduce L-DOPA-induced dyskinesia indirectly via ROCK inhibition (Carbajo-Lozoya et al., 2012). Statins (Wang et al., 2015) also induce inhibition of the RhoA/ROCK signalling (Nohria et al., 2009). Finally, amantadine has anti-inflammatory effects, in which ROCK may also be involved (Kim et al., 2012).

In conclusion, the present study shows that the ROCK inhibitor fasudil reduces the development of L-DOPA-induced dyskinesia and inhibits already established dyskinesia without affecting the therapeutic effect of L-DOPA. Interestingly, this compound may also protect the dopaminergic system against neuronal death. In addition to PD models, fasudil has been observed to exert beneficial effects in experimental models of Alzheimer's disease (Gu et al., 2018), Huntington's disease (Li et al., 2013) and amyotrophic lateral sclerosis (Gunther et al., 2017). A first clinical trial using fasudil in humans with neurodegenerative diseases has been started (Lingor et al., 2019). In clinical practice, fasudil has been used against vascular diseases since 1995 the safety and benefits of the compound are known (Suzuki, Shibuya, Satoh, Sugimoto, & Takakura, 2007). The present study suggests that fasudil is a good candidate for the treatment of L-DOPA-induced dyskinesia and may simultaneously exert neuroprotective effects against progression of PD.

ACKNOWLEDGEMENTS

AUTHOR CONTRIBUTIONS

A.M. and J.L.L.-G. designed the research and experiments; A.L.-L. and A.M. performed the experiments; A.M., J.L.L.-G. and C.M.L. contributed to writing, review critique; all authors edited the manuscript.

CONFLICT OF INTEREST

The authors declare no conflicts of interest.

DECLARATION OF TRANSPARENCY AND SCIENTIFIC RIGOUR

This Declaration acknowledges that this paper adheres to the principles for transparent reporting and scientific rigour of preclinical research as stated in the *BJP* guidelines for Design & Analysis, Immunoblotting and Immunochemistry and Animal Experimentation, and as recommended by funding agencies, publishers and other organizations engaged with supporting research.

DATA AVAILABILITY STATEMENT

The data that support the findings of this study are available from the corresponding author upon reasonable request. Some data may not be made available because of privacy or ethical restrictions.

ORCID

Andrea Lopez-Lopez https://orcid.org/0000-0002-1692-9637
Carmen M. Labandeira https://orcid.org/0000-0002-6274-5871
Jose L. Labandeira-Garcia https://orcid.org/0000-0002-8243-9791
Ana Muñoz https://orcid.org/0000-0002-7214-9774

REFERENCES

Alexander, S. P. H., Christopoulos, A., Davenport, A. P., Kelly, E., Mathie, A., Peters, J. A., ... Pawson, A. J. (2019). The Concise Guide to PHARMACOLOGY 2019/20: G protein-coupled receptors. *British Journal of Pharmacology*, 176(Suppl 1), S21–S141. https://doi.org/10.1111/bph.14748

Alexander, S. P. H., Roberts, R. E., Broughton, B. R. S., Sobey, C. G., George, C. H., Stanford, S. C., ... Ahluwalia, A. (2018). Goals and practicalities of immunoblotting and immunohistochemistry: A guide for submission to the *British Journal of Pharmacology*. *British Journal of Pharmacology*, 175, 407–411. https://doi.org/10.1111/bph.14112

Barcia, C., Ros, C. M., Annese, V., Carrillo-de Sauvage, M. A., Ros-Bernal, F., Gomez, A., ... Herrero, M. T. (2012). ROCK/Cdc42-mediated microglial motility and gliapse formation lead to phagocytosis of degenerating dopaminergic neurons in vivo. *Scientific Reports*, 2, 809. https://doi.org/10.1038/srep00809

Barnum, C. J., Eskow, K. L., Dupre, K., Blandino, P. Jr., Deak, T., & Bishop, C. (2008). Exogenous corticosterone reduces L-DOPA-induced dyskinesia in the hemi-parkinsonian rat: Role for interleukin-1β. *Neuroscience*, 156, 30–41. https://doi.org/10.1016/j.neuroscience.2008.07.016

Beattie, E. C., Stellwagen, D., Morishita, W., Bresnahan, J. C., Ha, B. K., Von Zastrow, M., ... Malenka, R. C. (2002). Control of synaptic strength by glial TNFα. *Science*, 295, 2282–2285. https://doi.org/10.1126/science.1067859

Boi, L., Pisanu, A., Greig, N. H., Scerba, M. T., Tweedie, D., Mulas, G., ... Carta, A. R. (2019). Immunomodulatory drugs alleviate L-dopa-induced dyskinesia in a rat model of Parkinson's disease. *Movement Disorders: Official Journal of the Movement Disorder Society*, 34, 1818–1830. https://doi.org/10.1002/mds.27799

Borrajo, A., Rodriguez-Perez, A. I., Diaz-Ruiz, C., Guerra, M. J., & Labandeira-Garcia, J. L. (2014). Microglial TNF-α mediates enhancement of dopaminergic degeneration by brain angiotensin. *Glia*, 62, 145–157. https://doi.org/10.1002/glia.22595

Borrajo, A., Rodriguez-Perez, A. I., Villar-Cheda, B., Guerra, M. J., & Labandeira-Garcia, J. L. (2014). Inhibition of the microglial response is essential for the neuroprotective effects of Rho-kinase inhibitors on MPTP-induced dopaminergic cell death. *Neuropharmacology*, 85, 1–8. https://doi.org/10.1016/j.neuropharm.2014.05.021

Bortolanza, M., Cavalcanti-Kiwiatkoski, R., Padovan-Neto, F. E., da-Silva, C. A., Mitkovski, M., Raisman-Vozari, R., & Del-Bel, E. (2015). Glial activation is associated with L-DOPA induced dyskinesia and blocked by a nitric oxide synthase inhibitor in a rat model of Parkinson's disease. *Neurobiology of Disease*, 73, 377–387. https://doi.org/10.1016/j.nbd.2014.10.017

Bryan, B. A., Dennstedt, E., Mitchell, D. C., Walshe, T. E., Noma, K., Loureiro, R., ... Patricia, D. A. A. (2010). RhoA/ROCK signaling is essential for multiple aspects of VEGF-mediated angiogenesis. *FASEB Journal*, 24, 3186–3195. https://doi.org/10.1096/fj.09-145102

Carbajo-Lozoya, J., Lutz, S., Feng, Y., Kroll, J., Hammes, H. P., & Wieland, T. (2012). Angiotensin II modulates VEGF-driven angiogenesis by opposing effects of type 1 and type 2 receptor stimulation in the microvascular endothelium. *Cellular Signalling*, 24, 1261–1269. https://doi.org/10.1016/j.cellsig.2012.02.005

Carta, M., Lindgren, H. S., Lundblad, M., Stancampiano, R., Fadda, F., & Cenci, M. A. (2006). Role of striatal L-DOPA in the production of dyskinesia in 6-hydroxydopamine lesioned rats. *Journal of Neurochemistry*Mar, 96(6), 1718–1727. https://doi.org/10.1111/j.1471-4159.2006.03696.x

Cenci, M. A., & Crossman, A. R. (2018). Animal models of L-dopa-induced dyskinesia in Parkinson's disease. *Movement Disorders: Official Journal of the Movement Disorder Society*, 33, 889–899. https://doi.org/10.1002/mds.27337

Cenci, M. A., & Konradi, C. (2010). Maladaptive striatal plasticity in L-DOPA-induced dyskinesia. *Progress in Brain Research*, 183, 209–233. https://doi.org/10.1016/S0079-6123(10)83011-0

Chen, M., Liu, A., Ouyang, Y., Huang, Y., Chao, X., & Pi, R. (2013). Fasudil and its analogs: A new powerful weapon in the long war against central nervous system disorders? *Expert Opinion Investigational Drugs*, 22, 537–550. https://doi.org/10.1517/13543784.2013.778242

Defert, O., & Boland, S. (2017). Rho kinase inhibitors: A patent review (2014–2016). *Expert Opinion on Therapeutic Patents*, 27, 507–515. https://doi.org/10.1080/13543776.2017.1272579

Espay, A. J., Morgante, F., Merola, A., Fasano, A., Marsili, L., Fox, S. H., ... Lang, A. E. (2018). Levodopa-induced dyskinesia in Parkinson disease: Current and evolving concepts. *Annals of Neurology*, 84, 797–811. https://doi.org/10.1002/ana.25364

Gerhard, A., Pavese, N., Hotton, G., Turkheimer, F., Es, M., Hammers, A., ... Brooks, D. J. (2006). In vivo imaging of microglial activation with [11C](R)-PK11195 PET in idiopathic Parkinson's disease. *Neurobiology of Disease*, 21, 404–412. https://doi.org/10.1016/j.nbd.2005.08.002

Gu, Q. F., Yu, J. Z., Wu, H., Li, Y. H., Liu, C. Y., Feng, L., ... Ma, C. G. (2018). Therapeutic effect of Rho kinase inhibitor FSD-C10 in a mouse model of Alzheimer's disease. *Experimental and Therapeutic Medicine*, *16*, 3929–3938. https://doi.org/10.3892/etm. 2018.6701

Gunther, R., Balck, A., Koch, J. C., Nientiedt, T., Sereda, M., Bahr, M., ... Tonges, L. (2017). Rho kinase inhibition with fasudil in the SOD1^{G93A} mouse model of amyotrophic lateral sclerosis—Symptomatic treatment potential after disease onset. *Frontiers in Pharmacology*, *8*, 17. https://doi.org/10.3389/fphar.2017.00017

Heasman, S. J., & Ridley, A. J. (2010). Multiple roles for RhoA during T cell transendothelial migration. *Small GTPases*, *1*, 174–179. https://doi.org/10.4161/sgtp.1.3.14724

Hoang, M. V., Whelan, M. C., & Senger, D. R. (2004). Rho activity critically and selectively regulates endothelial cell organization during angiogenesis. *Proceedings of the National Academy of Sciences of the United States of America*, *101*, 1874–1879. https://doi.org/10.1073/pnas. 0308525100

Honing, H., van den Berg, T. K., van der Pol, S. M., Dijkstra, C. D., van der Kammen, R. A., Collard, J. G., & de Vries, H. E. (2004). RhoA activation promotes transendothelial migration of monocytes via ROCK. *Journal of Leukocyte Biology*, *75*, 523–528. https://doi.org/10.1189/jlb. 0203054

Johnston, T. H., Lacoste, A. M. B., Visanji, N. P., Lang, A. E., Fox, S. H., & Brotchie, J. M. (2019). Repurposing drugs to treat L-DOPA-induced dyskinesia in Parkinson's disease. *Neuropharmacology*, *147*, 11–27. https://doi.org/10.1016/j.neuropharm.2018.05.035

Kim, J. H., Lee, H. W., Hwang, J., Kim, J., Lee, M. J., Han, H. S., ... Suk, K. (2012). Microglia-inhibiting activity of Parkinson's disease drug amantadine. *Neurobiology of Aging*, *33*, 2145–2159. https://doi.org/10.1016/j.neurobiolaging.2011.08.011

Koch, J. C., Tatenhorst, L., Roser, A. E., Saal, K. A., Tonges, L., & Lingor, P. (2018). ROCK inhibition in models of neurodegeneration and its potential for clinical translation. *Pharmacology & Therapeutics*, *189*, 1–21. https://doi.org/10.1016/j.pharmthera.2018.03.008

Labandeira-Garcia, J. L., Rodriguez-Perez, A. I., Villar-Cheda, B., Borrajo, A., Dominguez-Meijide, A., & Guerra, M. J. (2015). Rho kinase and dopaminergic degeneration: A promising therapeutic target for Parkinson's disease. *The Neuroscientist: A Review Journal Bringing Neurobiology, Neurology and Psychiatry*, *21*, 616–629. https://doi.org/10.1177/1073858414554954

Labandeira-Garcia, J. L., Rozas, G., Lopez-Martin, E., Liste, I., & Guerra, M. J. (1996). Time course of striatal changes induced by 6-hydroxydopamine lesion of the nigrostriatal pathway, as studied by combined evaluation of rotational behaviour and striatal Fos expression. *Experimental Brain Research*, *108*, 69–84. https://doi.org/10.1007/BF00242905

Lerner, R. P., Francardo, V., Fujita, K., Bimpisidis, Z., Jourdain, V. A., Tang, C. C., ... Eidelberg, D. (2017). Levodopa-induced abnormal involuntary movements correlate with altered permeability of the blood-brain-barrier in the basal ganglia. *Scientific Reports*, *7*, 16005. https://doi.org/10.1038/s41598-017-16228-1

Li, M., Yasumura, D., Ma, A. A., Matthes, M. T., Yang, H., Nielson, G., ... Diamond, M. I. (2013). Intravitreal administration of HA-1077, a ROCK inhibitor, improves retinal function in a mouse model of Huntington disease. *PLoS ONE*, *8*, e56026. https://doi.org/10.1371/journal.pone. 0056026

Lilley, E., Stanford, S. C., Kendall, D. E., Alexander, S. P., Cirino, G., Docherty, J. R., ... Ahluwalia, A. (2020). ARRIVE 2.0 and the *British Journal of Pharmacology*: Updated guidance for 2020. *British Journal of Pharmacology*. https://doi.org/10.1111/bph.15178

Lingor, P., Weber, M., Camu, W., Friede, T., Hilgers, R., Leha, A., ... Bidner, H. (2019). ROCK-ALS: Protocol for a randomized, placebo-controlled, double-blind phase IIa trial of safety, tolerability and efficacy of the Rho kinase (ROCK) inhibitor fasudil in amyotrophic lateral

sclerosis. *Frontiers in Neurology*, *10*, 293. https://doi.org/10.3389/fneur.2019.00293

Mair, K. M., MacLean, M. R., Morecroft, I., Dempsie, Y., & Palmer, T. M. (2008). Novel interactions between the 5-HT transporter, 5-HT$_{1B}$ receptors and Rho kinase in vivo and in pulmonary fibroblasts. *British Journal of Pharmacology*, *155*, 606–616. https://doi.org/10.1038/bjp. 2008.310

Moskal, N., Riccio, V., Bashkurov, M., Taddese, R., Datti, A., Lewis, P. N., & Angus McQuibban, G. (2020). ROCK inhibitors upregulate the neuroprotective Parkin-mediated mitophagy pathway. *Nature Communications*, *11*, 88. https://doi.org/10.1038/s41467-019-13781-3

Mulas, G., Espa, E., Fenu, S., Spiga, S., Cossu, G., Pillai, E., ... Spolitu, S. (2016). Differential induction of dyskinesia and neuroinflammation by pulsatile versus continuous L-DOPA delivery in the 6-OHDA model of Parkinson's disease. *Experimental Neurology*, *286*, 83–92. https://doi.org/10.1016/j.expneurol.2016.09.013

Muñoz, A., Garrido-Gil, P., Dominguez-Meijide, A., & Labandeira-Garcia, J. L. (2014). Angiotensin type 1 receptor blockage reduces L-dopa-induced dyskinesia in the 6-OHDA model of Parkinson's disease. Involvement of vascular endothelial growth factor and interleukin-1β. *Experimental Neurology*, *261*, 720–732. https://doi.org/10.1016/j.expneurol.2014.08.019

Muñoz, A., Li, Q., Gardoni, F., Marcello, E., Qin, C., Carlsson, T., ... Carta, M. (2008). Combined 5-HT$_{1A}$ and 5-HT$_{1B}$ receptor agonists for the treatment of L-DOPA-induced dyskinesia. *Brain*, *131*, 3380–3394. https://doi.org/10.1093/brain/awn235

Nakabayashi, H., & Shimizu, K. (2011). HA1077, a Rho kinase inhibitor, suppresses glioma-induced angiogenesis by targeting the Rho-ROCK and the mitogen-activated protein kinase kinase/extracellular signal-regulated kinase (MEK/ERK) signal pathways. *Cancer Science*, *102*, 393–399. https://doi.org/10.1111/j.1349-7006.2010.01794.x

Nohria, A., Prsic, A., Liu, P. Y., Okamoto, R., Creager, M. A., Selwyn, A., & Ganz, P. (2009). Statins inhibit Rho kinase activity in patients with atherosclerosis. *Atherosclerosis*, *205*, 517–521. https://doi.org/10.1016/j.atherosclerosis.2008.12.023

Ohlin, K. E., Francardo, V., Lindgren, H. S., Sillivan, S. E., O'Sullivan, S. S., Luksik, A. S., ... Cenci, M. A. (2011). Vascular endothelial growth factor is upregulated by L-dopa in the parkinsonian brain: Implications for the development of dyskinesia. *Brain*, *134*, 2339–2357. https://doi.org/10.1093/brain/awr165

Ohlin, K. E., Sebastianutto, I., Adkins, C. E., Lundblad, C., Lockman, P. R., & Cenci, M. A. (2012). Impact of L-DOPA treatment on regional cerebral blood flow and metabolism in the basal ganglia in a rat model of Parkinson's disease. *NeuroImage*, *61*, 228–239. https://doi.org/10.1016/j.neuroimage.2012.02.066

Olsson, M., Nikkhah, G., Bentlage, C., & Bjorklund, A. (1995). Forelimb akinesia in the rat Parkinson model: Differential effects of dopamine agonists and nigral transplants as assessed by a new stepping test. *Journal of Neuroscience*, *15*, 3863–3875.

Padovan-Neto, F. E., Cavalcanti-Kiwiatkoviski, R., Carolino, R. O., Anselmo-Franci, J., & Del Bel, E. (2015). Effects of prolonged neuronal nitric oxide synthase inhibition on the development and expression of L-DOPA-induced dyskinesia in 6-OHDA-lesioned rats. *Neuropharmacology*, *89*, 87–99. https://doi.org/10.1016/j.neuropharm.2014.08.019

Percie du Sert, N., Hurst, V., Ahluwalia, A., Alam, S., Avey, M. T., Baker, M., ... Würbel, H. (2020). The ARRIVE guidelines 2.0: Updated guidelines for reporting animal research. *PLoS Biology*, *18*(7), e3000410. https://doi.org/10.1371/journal.pbio.3000410

Pisanu, A., Boi, L., Mulas, G., Spiga, S., Fenu, S., & Carta, A. R. (2018). Neuroinflammation in L-DOPA-induced dyskinesia: Beyond the immune function. *Journal of Neural Transmission (Vienna)*, *125*, 1287–1297. https://doi.org/10.1007/s00702-018-1874-4

Rodriguez-Pallares, J., Parga, J. A., Muñoz, A., Rey, P., Guerra, M. J., & Labandeira-Garcia, J. L. (2007). Mechanism of 6-hydroxydopamine

neurotoxicity: The role of NADPH oxidase and microglial activation in 6-hydroxydopamine-induced degeneration of dopaminergic neurons. *Journal of Neurochemistry*, *103*, 145–156. https://doi.org/10.1111/j.1471-4159.2007.04699.x

Rodriguez-Perez, A. I., Borrajo, A., Rodriguez-Pallares, J., Guerra, M. J., & Labandeira-Garcia, J. L. (2015). Interaction between NADPH-oxidase and Rho-kinase in angiotensin II-induced microglial activation. *Glia*, *63*, 466–482. https://doi.org/10.1002/glia.22765

Rodriguez-Perez, A. I., Dominguez-Meijide, A., Lanciego, J. L., Guerra, M. J., & Labandeira-Garcia, J. L. (2013). Inhibition of Rho kinase mediates the neuroprotective effects of estrogen in the MPTP model of Parkinson's disease. *Neurobiology of Disease*, *58*, 209–219. https://doi.org/10.1016/j.nbd.2013.06.004

Rodriguez-Perez, A. I., Valenzuela, R., Villar-Cheda, B., Guerra, M. J., & Labandeira-Garcia, J. L. (2012). Dopaminergic neuroprotection of hormonal replacement therapy in young and aged menopausal rats: Role of the brain angiotensin system. *Brain*, *135*, 124–138. https://doi.org/10.1093/brain/awr320

Sakai, N., Kaufman, S., & Milstien, S. (1995). Parallel induction of nitric oxide and tetrahydrobiopterin synthesis by cytokines in rat glial cells. *Journal of Neurochemistry*, *65*, 895–902. https://doi.org/10.1046/j.1471-4159.1995.65020895.x

Schallert, T., & Tillerson, J. L. (1999). *Intervention strategies for degeneration of dopamine neurons in parkinsonism: Optimising behavioural assessment of outcome*. Clifton, NJ: Humana Press.

Soto-Otero, R., Méndez-Alvarez, E., Hermida-Ameijeiras, A., Muñoz-Patiño, A. M., & Labandeira-Garcia, J. L. (2000). Autoxidation and neurotoxicity of 6-hydroxydopamine in the presence of some antioxidants: Potential implication in relation to the pathogenesis of Parkinson's disease. *Journal of Neurochemistry*, *74*, 1605–1612. https://doi.org/10.1046/j.1471-4159.2000.0741605.x

Sun, H., Breslin, J. W., Zhu, J., Yuan, S. Y., & Wu, M. H. (2006). Rho and ROCK signaling in VEGF-induced microvascular endothelial hyperpermeability. *Microcirculation*, *13*, 237–247. https://doi.org/10.1080/10739680600556944

Suzuki, Y., Shibuya, M., Satoh, S., Sugimoto, Y., & Takakura, K. (2007). A postmarketing surveillance study of fasudil treatment after aneurysmal subarachnoid hemorrhage. *Surgical Neurology*, *68*, 126–131discussion 131–122. https://doi.org/10.1016/j.surneu.2006.10.037

Takeuchi, H., Jin, S., Wang, J., Zhang, G., Kawanokuchi, J., Kuno, R., … Suzumura, A. (2006). Tumor necrosis factor-α induces neurotoxicity via glutamate release from hemichannels of activated microglia in an autocrine manner. *The Journal of Biological Chemistry*, *281*, 21362–21368. https://doi.org/10.1074/jbc.M600504200

Tatenhorst, L., Tönges, L., Saal, K. A., Koch, J. C., Szegő, É. M., Bähr, M., & Lingor, P. (2014). Rho kinase inhibition by fasudil in the striatal 6-hydroxydopamine lesion mouse model of Parkinson disease. *Journal of Neuropathology and Experimental Neurology*, *73*, 770–779. https://doi.org/10.1097/NEN.0000000000000095

Teema, A. M., Zaitone, S. A., & Moustafa, Y. M. (2016). Ibuprofen or piroxicam protects nigral neurons and delays the development of L-dopa induced dyskinesia in rats with experimental Parkinsonism: Influence on angiogenesis. *Neuropharmacology*, *107*, 432–450. https://doi.org/10.1016/j.neuropharm.2016.03.034

Villar-Cheda, B., Dominguez-Meijide, A., Joglar, B., Rodriguez-Perez, A. I., Guerra, M. J., & Labandeira-Garcia, J. L. (2012). Involvement of microglial RhoA/Rho-kinase pathway activation in the dopaminergic neuron death. Role of angiotensin via angiotensin type 1 receptors. *Neurobiology of Disease*, *47*, 268–279. https://doi.org/10.1016/j.nbd.2012.04.010

Walsh, S., Finn, D. P., & Dowd, E. (2011). Time-course of nigrostriatal neurodegeneration and neuroinflammation in the 6-hydroxydopamine-induced axonal and terminal lesion models of Parkinson's disease in the rat. *Neuroscience*, *175*, 251–261. https://doi.org/10.1016/j.neuroscience.2010.12.005

Wang, T., Cao, X., Zhang, T., Shi, Q., Chen, Z., & Tang, B. (2015). Effect of simvastatin on L-DOPA-induced abnormal involuntary movements of hemiparkinsonian rats. *Neurological Sciences*, *36*, 1397–1402. https://doi.org/10.1007/s10072-015-2127-z

Winkler, C., Kirik, D., Bjorklund, A., & Cenci, M. A. (2002). L-DOPA-induced dyskinesia in the intrastriatal 6-hydroxydopamine model of Parkinson's disease: Relation to motor and cellular parameters of nigrostriatal function. *Neurobiology of Disease*, *10*, 165–186. https://doi.org/10.1006/nbdi.2002.0499

Wu, J., Li, J., Hu, H., Liu, P., Fang, Y., & Wu, D. (2012). Rho-kinase inhibitor, fasudil, prevents neuronal apoptosis via the Akt activation and PTEN inactivation in the ischemic penumbra of rat brain. *Cellular and Molecular Neurobiology*, *32*, 1187–1197. https://doi.org/10.1007/s10571-012-9845-z

Wu, Y., Dissing-Olesen, L., MacVicar, B. A., & Stevens, B. (2015). Microglia: Dynamic mediators of synapse development and plasticity. *Trends in Immunology*, *36*, 605–613. https://doi.org/10.1016/j.it.2015.08.008

Zhang, S., Gao, J., Huang, Y., & Xu, W. (2009). Study on the pharmacokinetics of fasudil, a selective Rho kinase inhibitor. *Asian Journal of Pharmacodynamics and Pharmacokinetics*, *9*(3), 221–226.